

Old Dominion University

ODU Digital Commons

Electrical & Computer Engineering Theses &
Dissertations

Electrical & Computer Engineering

Spring 1990

Hydrogenation Effects on Trap Related Conduction in Diamond

Linwood Cleveland Watkins III
Old Dominion University

Follow this and additional works at: https://digitalcommons.odu.edu/ece_etds



Part of the [Electronic Devices and Semiconductor Manufacturing Commons](#), and the [Engineering Science and Materials Commons](#)

Recommended Citation

Watkins, Linwood C.. "Hydrogenation Effects on Trap Related Conduction in Diamond" (1990). Master of Science (MS), Thesis, Electrical & Computer Engineering, Old Dominion University, DOI: 10.25777/kwva-sk96

https://digitalcommons.odu.edu/ece_etds/571

This Thesis is brought to you for free and open access by the Electrical & Computer Engineering at ODU Digital Commons. It has been accepted for inclusion in Electrical & Computer Engineering Theses & Dissertations by an authorized administrator of ODU Digital Commons. For more information, please contact digitalcommons@odu.edu.

HYDROGENATION EFFECTS ON TRAP RELATED
CONDUCTION IN DIAMOND

by


Linwood Cleveland Watkins III
B.S.E.E. May 1987, Old Dominion University

A Thesis Submitted to the Faculty of
Old Dominion University in Partial Fulfillment of the
Requirements for the Degree of

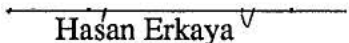
MASTER OF SCIENCE
ELECTRICAL ENGINEERING

OLD DOMINION UNIVERSITY
May, 1990

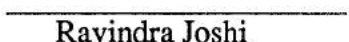
Approved by:



Sacharia Albin



Hasan Erkaya



Ravindra Joshi

ABSTRACT

**HYDROGENATION EFFECTS ON TRAP RELATED
CONDUCTION IN DIAMOND**

Linwood Cleveland Watkins III

Old Dominion University

Director: Dr. Sacharia Albin

In this research work, the results of an experimental investigation on the electrical conduction mechanism in type Ia and IIb diamonds are presented. These results are compared with those of previous theoretical studies. The basic physical properties of diamond are discussed. Details of ohmic contact formation on diamond are presented.

The current-voltage characteristics revealed the presence of traps located below the Fermi level. The unfilled trap density was determined. The deep traps were further studied using spectroscopic photoconductivity measurements and the trap energy levels were determined.

The effects of hydrogenation on trap related conduction were studied subsequently. Hydrogenation was carried out in both rf and microwave plasma and found to be a diffusion limited process, independent of plasma density. Upon hydrogenation the conductivity of diamond samples increased by ten orders of magnitude, which was shown to be due to the passivation of deep traps by hydrogen. The amount of hydrogen introduced into the diamond was determined. It is concluded that the performance of diamond devices will be significantly affected by hydrogenation.

Acknowledgements

I would first like to thank Dr. Sacharia Albin. His help, patience, and friendship have made my education a truly enjoyable experience. Special thanks also go to Dr. Hasan Erkaya and Dr. Ravindra Joshi for their time and assistance in bringing this research to a close.

Thanks also go to Jim Satira for his time and programming expertise. Working with him made those long days in lab almost bearable.

Most important, I would like to thank my wife, Melinda. She pushed and sometimes dragged me down the road to completion. I know it wasn't easy but I'm glad she stuck it out with me. Thanks!

I would also like to thank my family for the years of support they have given me.

Finally, I would like to acknowledge the NASA Graduate Research Fellowship Program without whose financial support this work would not have been completed.

TABLE OF CONTENTS

	PAGE
List of Figures	v
List of Graphs	vi
Chapter	
1. Introduction	1
General Properties of Diamond	1
Mechanical Properties of Diamond	2
Thermal Properties of Diamond	2
Optical Properties of Diamond	3
Electrical Properties of Diamond	4
Chemical Properties of Diamond	4
Scope of Research	5
2. Contact and Sample Preparation	6
Metal-Semiconductor Contacts	6
Contact Deposition	12
3. DC Current-Voltage Characteristics	13
Theory of Current Injection	13
Trap Free Square Law	13
Trap Free Case with Thermal Free Carriers	14
Charge Conduction in the Presence of Traps	16
Shallow Traps	17
Deep Traps	18

Experimental Results	21
Type Ia Diamond	24
Type IIb Diamond	24
Discussion	28
4. Photoconductivity in Semiconductors	30
Theory of Photoconductivity	30
Fundamental Photoconductivity	31
Impurity Photoconductivity	32
Experimental Results	36
Type Ia Diamond	39
Type IIb Diamond	39
Discussion	42
5. Effects of Hydrogenation in Diamond	46
Effects of Hydrogenation in Semiconductors	46
Experimental Results	47
Type Ia Diamond	47
Type IIb Diamond	49
Discussion	53
6. Summary and Conclusions	58
Current-Voltage Characteristics of Diamond	58
Photoconductivity of Diamond	58
Hydrogenation Effects in Diamond	59
Future Research	60
References	61

LIST OF FIGURES

FIGURE	PAGE
1. Metal semiconductor interface a) large separation b) electrically connected and c) intimate contact	7
2. Surface states on a semiconductor	9
3. Conduction at a metal semiconductor interface a) thermionic emission, b) thermionic-field emission and c) field emission	11
4. Current-voltage characteristics a) shallow trap and b) deep trap	20
5. I-V measurement system	22
6. Photoconductivity in semiconductors a) band structure and b) photoconductive spectrum	34
7. Photoconductivity measurement system	37
8. Band diagram for a semiconductor containing a deep trap	55

LIST OF GRAPHS

GRAPH	PAGE
1. I-V characteristics of type Ia diamond	25
2. I-V characteristics of type IIb diamond	27
3. Emission spectrum for xenon arc lamp	38
4. Uncorrected photoconductivity spectrum for type Ia diamond	40
5. Corrected photoconductivity spectrum for type Ia diamond	41
6. Uncorrected photoconductivity spectrum for type IIb diamond	43
7. Corrected photoconductivity spectrum for type IIb diamond	44
8. I-V characteristics of type Ia diamond hydrogenated in rf plasma	48
9. I-V characteristics of type Ia diamond hydrogenated in microwave plasma	50
10. I-V characteristics of type IIb diamond hydrogenated in microwave plasma	51
11. Hydrogen content versus time	52
12. I-V characteristics of type IIb diamond after four hours of Hydrogenation	56

CHAPTER 1

INTRODUCTION

It is said that "Diamonds are a woman's best friend", however, due to the unique combination of optical, mechanical, thermodynamic and electrical properties of this material, one could say that diamonds are a scientist's best friend, too. The research interest in diamond has grown dramatically since the founding of the Diamond Research Laboratory, South Africa, in the late 1940's. In addition to the studies on the mechanical properties of diamond for tools, drill bits and abrasives, the laboratory began researching its crystalline, optical and electrical properties.

1.1 General Properties of Diamond

Diamond is composed of the single element carbon. The carbon atoms are arranged in a crystal lattice such that each carbon atom is bonded to four others with a singular covalent bond. The crystal structure is a diamond lattice with eight atoms per unit cell and cubic space group symmetry. The lattice constant of diamond is 0.3567 nm and it has a number density of 1.77×10^{23} atoms per cubic centimeter [1].

In addition to carbon atoms in the lattice, nitrogen and boron have also been found to be incorporated into a lattice site. Nitrogen is present in all natural diamonds with up to 0.2% in some type Ia diamonds. Boron is found with concentrations up to 0.5 ppm in rare natural type IIb diamonds and can be doped as high as 300 ppm in synthetic type IIb diamonds. Other impurities, such as transition metals, are frequently found in both synthetic and natural diamonds, however they are not incorporated into the crystal lattice

but occur in the form of inclusions, which do not affect the electrical properties of the diamond.

1.2 Mechanical Properties of Diamond

Diamond is the hardest material known to man. Its scratch hardness (10 on the Mohs scale) and indentation hardness (9000 kg mm^{-2}) are the highest known [2]. These properties make the surface of the diamond crystal very difficult to damage. The crystal itself, however, can be cleaved with relative ease and thus damage to gemstones is not impossible.

Another mechanical property of diamond which makes it invaluable to industry is its coefficient of friction. In air, the coefficient of friction of diamond on diamond is extremely low, between 0.05 and 0.1, depending on the orientation. This feature has already been used to produce good quality diamond on diamond bearings for motors to achieve high efficiency. Bearing lifetime is extended due to the low coefficient of friction and low wear rate of diamond.

In contrast, the coefficient of friction of diamond on metals is extremely high, 1 to 3. Diamonds are used as abrasives on softer materials due to this high coefficient of friction. When the friction force is greater than the shear strength of the softer material, the surface of the metal is abraded [1]. Using various sizes of diamond particles, surfaces can be polished to a mirror finish with sub micron tolerances.

1.3 Thermal Properties of Diamond

Perhaps, one of the most remarkable properties of diamond is its thermal conductivity. Diamond's thermal conductivity is five times that of copper. As a result, one of the most important uses for diamonds is as heat sinks. As semiconductor diode lasers were being developed, it became obvious that the major factor limiting the maximum output power was the rate at which the heat from the device could be carried away. Initially,

copper was used as the heat sink material but as the output power was increased, the thermal conductivity of copper was no longer sufficient. Diamond heat sinks, though, have allowed diode lasers to operate at 1 Watt CW power and beyond.

Another potential use for diamond's high thermal conductivity has been in the area of protective coatings for optical elements. Preliminary studies show that the laser damage threshold of materials can be increased dramatically by coating them with a layer of polycrystalline diamond film [3]. The diamond film serves to dissipate the heat from the surface of the protected material and thus increases the threshold due to thermal breakdown.

1.4 Optical Properties of Diamond

Diamond is an indirect bandgap material. This implies that for an electron to move from the top of the valence band to the conduction band minima, a change in momentum is required. This can occur through nonradiative processes, where the phonons conserve the excess momentum, or via a radiative recombination center. The recombination center allows most of the electron energy to go into the emission of a photon while, the momentum is absorbed into the lattice in the form of phonons. Color centers provide one such path for radiative emission in diamonds.

Because of the wide bandgap, diamonds are transparent over a broad region of the electromagnetic spectrum. Although there is some absorption due to impurities and defects, a good quality diamond will be optically transparent between 225 nm and 2.5 mm and beyond 6 mm. This optical transparency has made diamond an excellent window for spectrometer systems.

1.5 Electrical Properties of Diamond

Pure diamond is an excellent insulator at room temperature. Type IIa diamonds, with low concentrations of nitrogen, can have resistivities greater than 10^{16} ohm cm. In

1952, Custers observed diamond which had a much larger electrical conductivity than had been found previously [4]. This type of diamond was found to be p type semiconducting with resistivities as low as 10 ohm cm. This class of diamond was referred to as type IIb. The occurrence of type IIb diamonds in nature is rare. However, with the onset of high temperature, high pressure synthetic processes, type IIb bulk diamond can be manufactured with relative ease. Thin films of diamond can be doped during the growth process, which can then be incorporated into semiconductor devices.

Diamond has many advantages over other semiconducting materials. Because of its wide bandgap, 5.47 eV, thermal generation of carriers does not become appreciable until very high temperatures. While Si and GaAs devices can not operate beyond 150°C, diamond devices can operate relatively noise free up to about 700°C.

Another property which gives diamond an advantage over other semiconductors is its carrier mobilities. While Si has a wide difference in electron and hole mobilities, 1900 and 500 cm²/V·s, diamond has nearly equal mobilities, 1800 and 1500 cm²/V·s, respectively. Devices made with n type diamond would have nearly the same electrical characteristics as a p type device. Hence complementary metal oxide semiconductor (CMOS) type devices in diamond should have a higher speed than a corresponding Si CMOS device.

1.6 Chemical Properties of Diamond

Diamond is extremely chemically inert. The only materials which are able to attack diamond are those which, at high temperatures, act as oxidizing agents. Boiling sodium nitrate at 400°C will etch the diamond. Diamond can also be etched in oxygen at 600°C [2]. This inert behavior allows diamond to be used in extreme environments that would destroy most other materials.

1.7 Scope of Research

The objectives of this research are two-fold. The first is to study and characterize the electrical conduction mechanisms in bulk diamond. The potential applications of diamond in the field of electronics range from the areas of high temperature transistors to nuclear radiation detectors [5]. Therefore, it is important to understand the conduction mechanisms in diamond. Current-voltage (I-V) characteristics will be investigated. I-V studies will reveal the presence of traps within the semiconductor bandgap. Impurity photoconductivity will be used to identify the trap energies and the relative densities of each trap if more than one is present within the crystal. Impurity photoconductivity has been well studied in semiconductors and the theoretical background will be presented.

The second objective is to study the changes in conduction when the diamond is exposed to a hydrogen plasma. Atomic hydrogen has been shown to have significant effects on the electrical and optical characteristics of group IV and III-V semiconductors [6]. Diamond being another group IV semiconductor, should show similar effects and will be studied in detail.

CHAPTER 2

CONTACT AND SAMPLE PREPARATION

In this chapter, details of sample preparation, including etching and cleaning of the samples and deposition of the metal contacts, will be given. The general theory of ohmic contact formation on diamond will also be discussed. Finally, the sample preparation and contact formation used in the study will be discussed along with a description of actual contact behavior and how it pertains to the metal-semiconductor contact theory.

2.1 Metal-Semiconductor Contacts

The ideal ohmic metal-semiconductor contact is one in which charge carriers of either type, holes or electrons, are allowed to flow in either direction, from metal to semiconductor and vice versa, without impeding the flow. But, ideal ohmic contacts are not possible in actual devices due to the formation of a potential barrier at the interface [7].

Potential barriers are formed when two materials, with different work functions, are brought together in intimate contact in the absence of any surface states. As the metal and semiconductor are brought together, a transfer of charge takes place until the Fermi levels of the two materials line up. This can be seen for the case of an n-type semiconductor and a metal, with a larger work function, in Figure 1.

In Figure 1a, the two materials are shown with a large physical separation between them. The work functions, ϕ_m and ϕ_s , are for the metal and semiconductor respectively, where $\phi_m > \phi_s$. If the metal is electrically connected with a wire to the semiconductor, electrons will flow from the semiconductor into the metal until the two Fermi levels align,

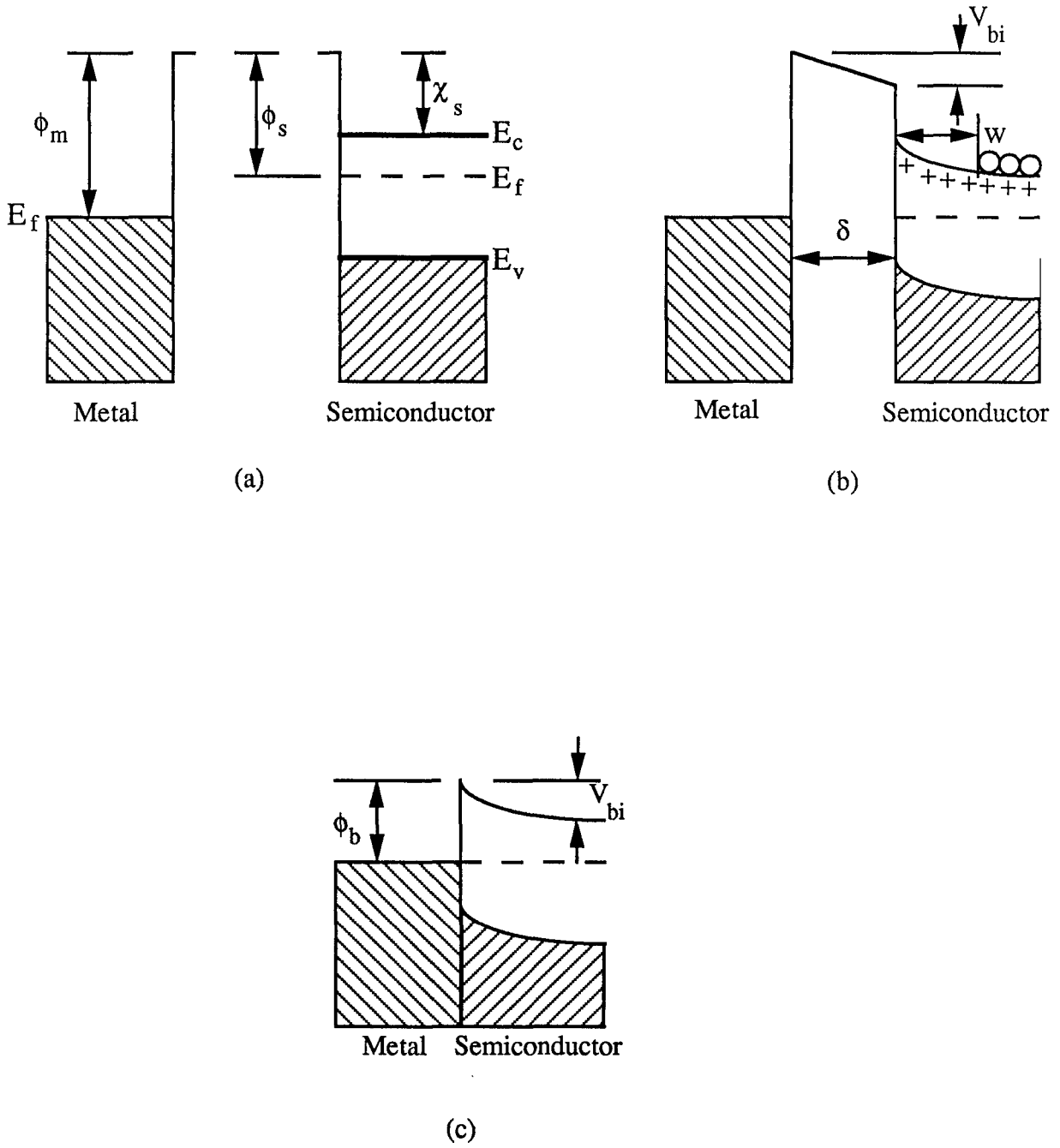


Figure 1. Metal Semiconductor Interface (a) Large Separation (b) Electrically Connected and (c) Intimate Contact

as shown in Figure 1b. The positively charged donors, formed in the semiconductor by the migration of electrons to the metal, are balanced by an equal negative charge on the surface of the metal. This creates an electric field in the region between the two materials. Because the doping concentration of the semiconductor is much less than the free electron concentration in the metal, the space charge region in the semiconductor is much greater than that of the metal and thus the bands of the semiconductor will bend. As the two materials are brought closer together the difference in potential of the two surfaces, V_i , must approach zero.

At the point where the metal and semiconductor meet, V_i becomes zero and the barrier which impedes the flow of electrons from the metal to the semiconductor is given by

$$\phi_b = \phi_m - \chi_s \quad (1)$$

where χ_s is the electron affinity of the semiconductor. The barrier which impedes the flow of electrons from the semiconductor to the metal is the built-in potential, V_{bi} and is given by

$$V_{bi} = \phi_m - \phi_s \quad (2)$$

This type of barrier is called a Schottky barrier (Figure 1c).

The effects of surface states on the barrier height must also be discussed. If the density of surface states is large, the barrier heights can differ from those given in equations (1) and (2), due to the effects of Fermi level pinning [8]. With very high densities of surface states, the barrier height can become independent of the metal work function.

To better understand this, assume that the metal and semiconductor are separated by a thin insulating layer, a native oxide, and that the semiconductor contains a distribution of traps which are uniformly spaced in energy and homogeneous across the surface. This distribution of surface states is characterized by a density, N_{ss} ($\text{cm}^{-2} \text{eV}^{-1}$), and a neutral level ϕ_0 (Figure 2). In the absence of surface states, the negative charge on the metal, Q_m is equal and opposite to the positively charged donors in the depletion region, Q_d . In the

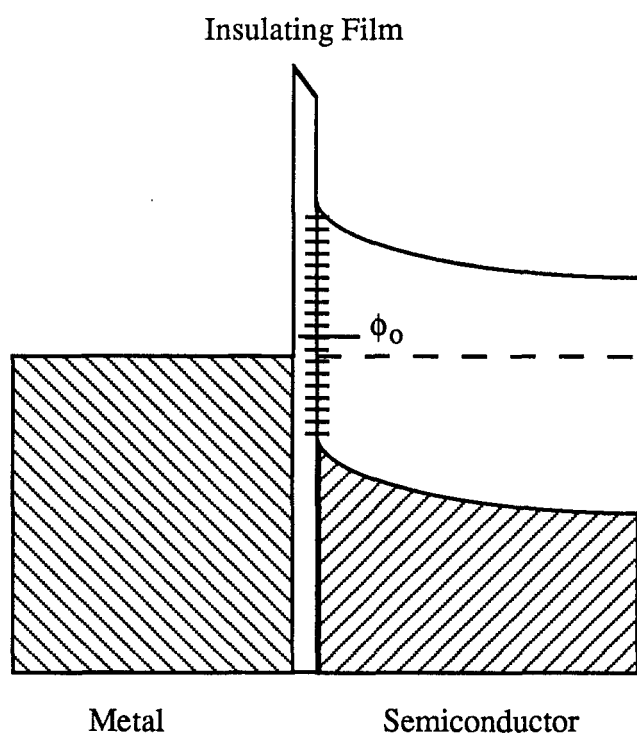


Figure 2. Surface States on a Metal-Semiconductor Interface

presence of surface states, this neutrality condition becomes $Q_m + Q_d + Q_{ss} = 0$, where Q_{ss} is the net charge stored in the surface states. If the Fermi level is below the neutral level, ϕ_0 the surface states contain a net positive charge, thus Q_d must be reduced by the same amount. This leads to a corresponding reduction in the depletion width and a reduction in the barrier height. This reduction in the barrier height pushes the neutral level toward the Fermi level and reduces the positive charge stored in the surface states.

If the density of the surface states is sufficiently high, the neutral level will be pushed very close to the Fermi level. In this case, the barrier height is given by $\phi_b = E_g - \phi_0$, where E_g is the bandgap of the semiconductor. The barrier height is said to be 'pinned' by the high density of surface states, and is independent of the metal work function.

The conduction through the metal-semiconductor contact is determined from the barrier height and the depletion width. The conduction through such a contact is determined by the type of charge transport taking place (Figure 3).

1. Thermionic Emission - The charge carriers are thermalized over the barrier.
2. Thermionic-Field Emission - The energetic carrier tunnel through the top of the barrier.
3. Field Emission - The barrier is narrow enough for the carriers to tunnel through the entire barrier.

The type of charge transport taking place is dependent on the doping of the semiconductor. For low doped materials, the barrier is too wide for tunneling to take place and thus thermionic emission is most common. As the doping is increased, the barrier width is reduced and the carrier begins to tunnel through the top of the barrier. This is called thermionic-field emission because it is a combination of thermionic emission and tunnelling mechanisms. For the case of highly doped materials, the depletion width is so narrow the carriers are able to tunnel through the barrier. This mechanism is called field emission and is described through quantum mechanics.

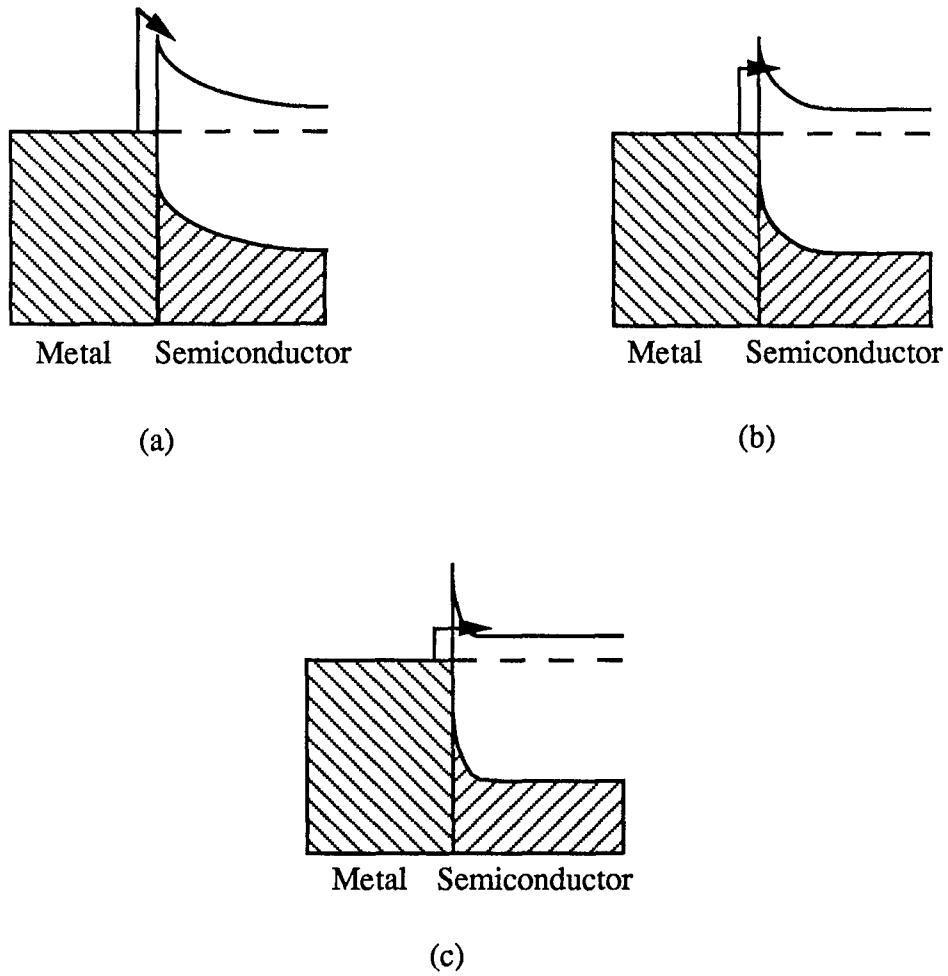


Figure 3. Conduction Across a Metal-Semiconductor Interface (a) Thermionic Emission (b) Thermionic-Field Emission and (c) Field Emission.

2.2 Contact Deposition

The contacts used in this study were made using a silver epoxy. Silver has been shown to form good ohmic contacts on diamond [9], and the contacts on these samples displayed excellent ohmic behavior.

The contacts were placed on opposite parallel faces of the diamond samples. Each contact was of the same size as the opposite contact, approximately 1 mm^2 in area. The contacts were placed in the center of the diamond face away from the edges to minimize surface leakage currents around the side of the diamonds.

CHAPTER 3

DC CURRENT-VOLTAGE CHARACTERISTICS

The theory of space charge limited current injection was first addressed in 1940 by N. F. Mott and R. W. Gurney [10]. In their book, "Electronic Processes in Ionic Crystals," they developed the theory that electrons could be injected into wide bandgap material. This injection theory, called space charge limited (SCL) conduction, was further developed by M. A. Lampert and P. Mark in 1970, and will be discussed here in detail [11]. Single carrier injection will also be discussed, due to its applicability to conduction in diamonds.

3.1 Theory of Current Injection

3.1.1 Trap Free Square Law

In deriving the "trap free square law", two assumptions are made. The first assumption is that there are no traps within the material and the second states that the thermal free carrier concentration is zero. The electron current density in an isotropic solid is given by

$$J = qn v_{\text{drift}} \quad (3.1)$$

where q is the electronic charge, n is the injected carrier concentration, and v_{drift} is the drift velocity of the charge carriers in the applied electric field. Assuming a linear relationship with the applied electric field, E , the drift velocity is given by

$$v_{\text{drift}} = \mu E \quad , \quad (3.2)$$

where μ is the mobility. Combining equations (3.1) and (3.2) with Poisson's equation, yields,

$$\frac{\epsilon}{q} \left(\frac{dE}{dx} \right) = n, \quad (3.3)$$

where ϵ is the permittivity of the semiconductor. This leads to the equation

$$E \left(\frac{dE}{dx} \right) = \frac{J}{\epsilon\mu}. \quad (3.4)$$

After integrating equation (3.4), subject to the initial condition that the electric field at the surface of the semiconductor is zero and evaluating at x equal to the thickness of the semiconductor, L , we get

$$V(L) = \sqrt{\frac{8J}{9\epsilon\mu}} L^{\frac{3}{2}}. \quad (3.5)$$

Rearranging (3.5), the Mott-Gurney equation is found

$$J = (9/8) \epsilon\mu (V^2 / L^3). \quad (3.6)$$

From the Mott-Gurney equation it can be seen that the injected current density is inversely proportional to the cube of the sample thickness and proportional to the square of the applied voltage. As a result, conduction which follows this behavior is referred to as being in the square law or space charge limited (SCL) region.

3.1.2 Trap Free Case with Thermal Free Carriers

The next step in the derivation of the conduction in solids is the introduction of thermal free carriers. Thermal free carriers are generated due to the thermodynamic tail of carriers which have sufficient energy to be excited into the conduction band of the material. The number of carriers can be calculated using Fermi statistics. The thermally generated carriers contribute to the current but not to the space charge.

Using Fermi statistics one can identify an energy at which the probability of occupation is 50%. This energy is called the Fermi level. The probability density function given by Fermi-Dirac statistics is

$$f(E) = \frac{1}{1 + \exp \left[\frac{E - F_o}{kT} \right]} , \quad (3.7)$$

where E is the energy under investigation, k is Boltzmann's constant, F_o is the Fermi level, and T is the absolute temperature. When $E_c - F_o \ll 4kT$ then the density function can be approximated by

$$f(E) = \exp \left[\frac{F_o - E}{kT} \right] . \quad (3.8)$$

The concentration of electron in the conduction band can be found using Fermi statistics and integrating

$$n_o = \int_{E_{c,min}}^{E_{c,max}} f(E) N(E) dE , \quad (3.9)$$

where n_o is the equilibrium electron concentration in the conduction band, $E_{c,min}$ and $E_{c,max}$ are the energies corresponding to the bottom and top of the conduction band, and $N(E) dE$ is the density of states in the range dE . This integral can be simplified using an effective density of states N_c located at the conduction band edge E_c . The equilibrium electron concentration becomes

$$n_o = N_c \exp \left[\frac{-(E_c - F_o)}{kT} \right] . \quad (3.10)$$

Until the injected charge, n_i , becomes comparable to the free carrier concentration, n_o , the thermal carriers will dominate the conduction mechanism and no space charge effects will be seen. The current density in this thermally free carrier dominated region will behave according to Ohm's Law. This region, therefore, is called the Ohmic region and the current density will be

$$J = qn_o\mu(V/L) . \quad (3.11)$$

Until the average injected charge density exceeds this value of n_o , a departure from Ohm's law will not be seen. The voltage at which the injected charge exceeds the thermal charge concentration is given by

$$V_x = (4/3) qn_o L^2 / \epsilon . \quad (3.12)$$

At a voltage greater than V_x , the current density will be given by the Mott-Gurney equation, (3.6). The current will then follow a square law dependence on the voltage.

3.1.3 Charge Conduction in the Presence of Traps

The presence of traps in the bulk of the semiconductor will, in general, decrease the current at low injection levels. The majority of the injected carriers will be captured by the traps in the bulk and will not contribute to the conduction current. Again, using Fermi-Dirac statistics, the concentration of filled traps at a level E_t is given by

$$n_{t,o} = \frac{N_t}{1 + \frac{1}{g} \exp \left[\frac{E_t - F_o}{kT} \right]} \quad (3.13)$$

where N_t is the trap concentration and g is the degeneracy factor for the trap. As carriers are trapped and re-emitted to the conduction band, a thermodynamic balance is reached corresponding to Fermi statistics at a characteristic temperature. Once this balance has been established, electron capture and emission rates from the trap will be equal.

If a field is applied to the sample, the balance between free and trapped charges is altered due to the additional injected charges. After sufficient time for the transients to die out, the semiconductor is again in thermal equilibrium with a new value of the free electron concentration n , under the injection conditions, and not the initial thermal equilibrium value n_o . This new thermodynamic equilibrium corresponds to a new Fermi level, F , called the quasi-Fermi level. The free electron concentration under injection is given by

$$n = n_i + n_o = N_c \exp \left[\frac{F - E_t}{kT} \right] \quad (3.14)$$

where n_i is the average excess injected charge concentration. The trapped electron concentration is given in a similar fashion as

$$n_t = n_{t,i} + n_{t,o} = \frac{N_t}{1 + \frac{1}{g} \exp \left[\frac{E_t - F}{kT} \right]} \quad (3.15)$$

where $n_{t,i}$ is the average excess injected trapped charge concentration and $n_{t,o}$ is the initial equilibrium trapped concentration.

Traps in the bulk of a semiconductor are categorized into two types depending on their position in the band structure with respect to the Fermi level.

3.1.4 Shallow Traps

An electron trap is said to be shallow if F , the Fermi level, lies below E_t , so that $(E_t - F) > kT$. From equations (3.14) and (3.15), a ratio of conduction electrons to trapped electrons can be found,

$$\frac{n}{n_t} = \frac{N_c}{gN_t} \exp\left(\frac{E_t - E_c}{kT}\right) = \Theta, \quad (3.16)$$

where Θ is a constant, independent of the injection level, as long as the trap remains shallow.

At sufficiently low voltages, Ohm's law will still be observed due to the presence of thermal free carriers. As the injection of carriers increases, there is a point at which the number of untrapped injected carriers exceeds the thermally free concentration and a crossover to the square-law regime will be observed. The voltage, V_x , at which this change over will take place is greater than that of the trap free case. This is due to the reduction in the number of conduction electrons caused by trapping. V_x is given by

$$V_x = (4/3) q n_0 L^2 / \Theta \epsilon. \quad (3.17)$$

Beyond this change over voltage, the current will follow a square law dependence on the voltage. By substituting the result $n = n_t \Theta$, into equation (3.1) and re-deriving, a new expression for the current density in the space charge limited region is given

$$J = (9/8) \Theta \epsilon \mu (V^2 / L^3). \quad (3.18)$$

3.1.5 Deep Traps

An electron trap is said to be deep if the Fermi level is above the trap energy, and $(F - E_t) > kT$. From equation (3.13), an expression for the concentration of traps not occupied by electrons is given by

$$p_{t,o} = N_t - n_{t,o} = \frac{N_t}{1 + g \exp\left[\frac{F_o - E_t}{kT}\right]} \quad (3.19)$$

As in the shallow trap case, the current voltage behavior will follow Ohm's law up to the point where the injected charge concentration becomes comparable to the thermal free carrier concentration. At this point, the quasi-Fermi level has shifted upward by an amount equal to $0.7kT$. This shift is sufficient to fill the remaining deep traps. The voltage corresponding to this complete filling of the traps is given by

$$V_{TH} = \frac{Q_{TH}}{C_o} = \frac{qp_{t,o}L}{C_o} = \frac{qp_{t,o}L^2}{2\epsilon} \quad (3.20)$$

where Q_{TFL} is the charge injected into the semiconductor at the voltage V_{TFL} and C_o is the geometric capacitance per unit area of the sample.

The changes in current beyond V_{TFL} are easily seen by looking at the effect of doubling the voltage to $2V_{TFL}$. Due to the relationship between charge and voltage, as the voltage is doubled, the injected charge is also doubled. Because the traps were filled at V_{TFL} , this additional injected charge must appear entirely in the conduction band, which equals $qp_{t,o}L$. Solving for the ratio of the current densities at $2V_{TFL}$ and V_{TFL}

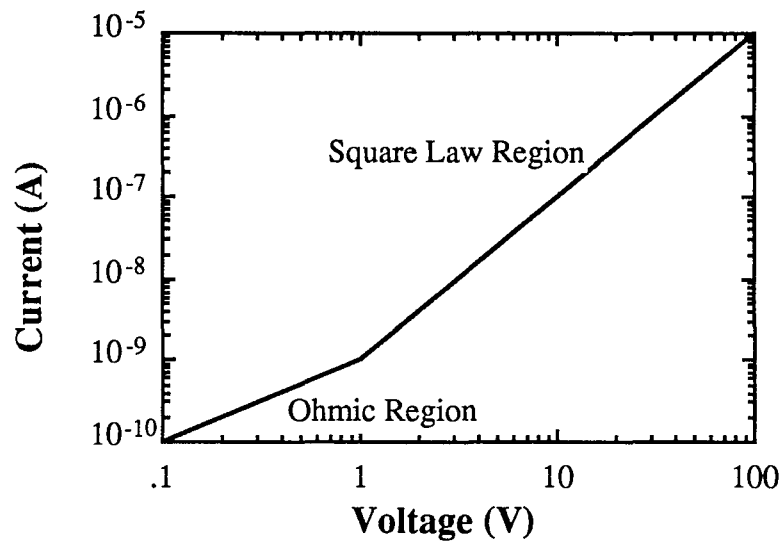
$$\frac{J(2V_{TH})}{J(V_{TH})} = \frac{p_{t,o}}{n_o} \quad (3.21)$$

is given. From this it can be seen that for highly insulating materials, the result of doubling the voltage can be an increase in the current density by several orders of magnitude.

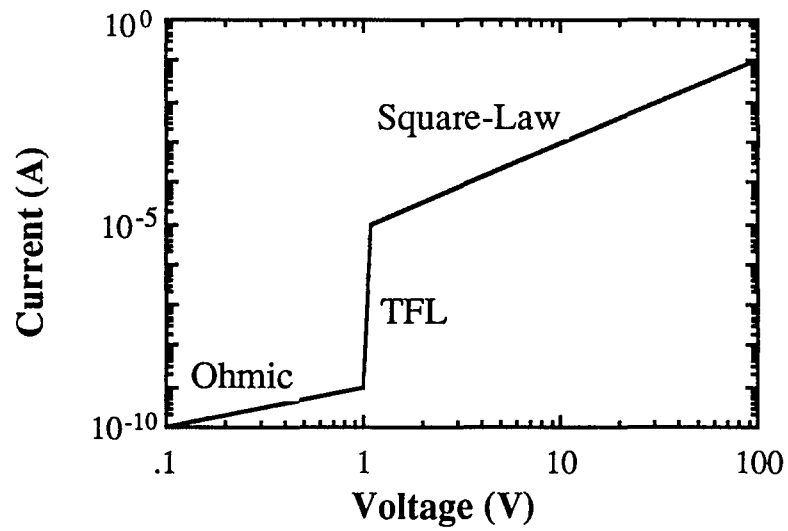
In Figure 4a, a single trap is present which is above the Fermi level. At low voltages, the current rises linearly with the voltage, due to the dominance of the thermal free carrier concentration. At the voltage V_x , the point at which the injected charge density equals the thermal free charge density, the conduction enters the space charge limited regime. This square law increase in the current continues until the quasi-Fermi moves above the trap energy level. At this point, the traps are filled and the current has a near

vertical transition up to the trap free square law curve. With further increases in the voltage, the current follows the trap free square law.

The second case is one in which a single set of deep traps exist. As can be seen in Figure 4b, the current begins increasing linearly with the voltage. As the voltage is further increased, there comes a point $V=V_{\text{TFL}}$ at which the current begins a sharp rise. The amount of increase in the current is proportional to the ratio of the initially unfilled traps to the thermal free carrier concentration. At a voltage of $2V_{\text{TFL}}$, the current merges with the trap free square law. The injected free charge density dominates the injected trapped charge density and any further injected carriers go into the conduction current.



(a)



(b)

Figure 4. Current-Voltage Characteristics (a) Shallow Trap and (b) Deep Trap.

3.2 Experimental Results

In order to obtain the I-V characteristics for insulators or wide bandgap semiconductors, extremely sensitive current measurements must be made. In order to achieve the sensitivity necessary, a Keithley 617 electrometer was used. The Keithley electrometer can accurately measure currents down to 10^{-14} A, with a resolution of 0.1 fA.

In order to minimize the error in the measurements, three possible causes of error had to be addressed. The most significant cause of error in low current measurements is due to electromagnetic interference (EMI) or noise. In order to reduce EMI, a double shielded test sample holder was designed (see Figure 5). The design is similar to a Faraday cage in which the inner and outer shields are tied to the experimental ground. Through electromagnetic theory, it can be shown that no electromagnetic waves can penetrate into the box. The waves are reflected from the zero impedance of the box. Prior to shielding the sample, small movements within the room were enough to induce large erroneous signals on the meter. After constructing the shielded enclosure, no such errors were seen.

The second type of error is due to the random component of the measured signal. Even though the test sample was shield from interference, a small, random component of the signal was observed. This was due to a combination of actual noise on the voltage signal and a random error induced by the measurement device. Both components of this random error could be minimized by averaging the signal over time.

In order to determine the number of readings needed to eliminate this error, the bias of the sample was fixed. The values from the meter were plotted without any averaging so that the amount of the error could be quantified. The random error measured ranged from 2 to 20% depending upon the magnitude of the current. Since the maximum error occurred at the lowest current level, 10^{-14} A, this was chosen as the operating point for optimization of averaging. The measurement was again repeated while averaging for various numbers of readings. The current was taken every 1/3 of a second, the maximum conversion rate for the meter. Beyond 20 readings per data point, no further decrease in the fluctuation of

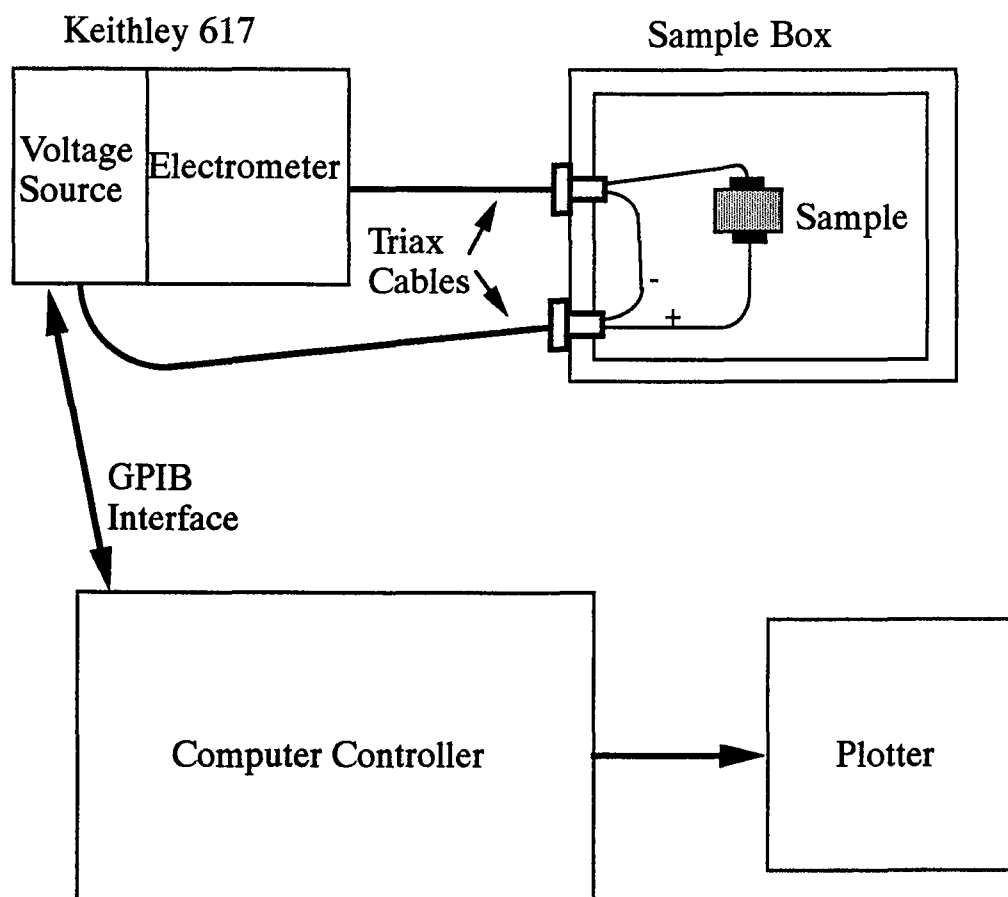


Figure 5. I-V Measurement System

values was apparent, so, 20 samples was chosen as the optimum. The random error after averaging was reduced from 20 to 3%.

The third type of error in this measurement is experimental or systematic error. This error is due to inconsistencies in the measurement technique. Changing the time interval between data points, changing the number of samples per point, or misreading data values from the meter are all forms of experimental error. Since humans are far apt to have more experimental errors than computers, it was decided that automating the data acquisition would minimize this error. The Keithley 617 electrometer is fully programmable over a general purpose interface bus (GPIB). After installing a GPIB interface card into the computer, a program was written in Pascal to control the meter and voltage source, retrieve the data from the meter, calculate the averages and plot the data. The data acquisition procedure is as follows:

1. The resistance of the sample is measured by the meter. Using an approximate capacitance, determined from the sample geometry, an approximate charging time constant can be calculated.
2. The voltage source applies the appropriate bias to the sample.
3. After a delay of five time-constants, the current through the sample is measured.
4. The current is sampled 20 times and the average is calculated, thus reducing the noise component of the signal.
5. The voltage is then increased and steps 2 through 4 are repeated.
6. The data is then written to a file for graphing.

Using this I-V measurement system, currents can be accurately determined over the range from 10 fA to 2 mA and resistances from 100 to 10^{16} Ohms. In addition to measuring the current, the resistance of the sample is calculated at each bias point and these values can be used to determine the resistivity of the sample.

3.2.1 Type Ia Diamond

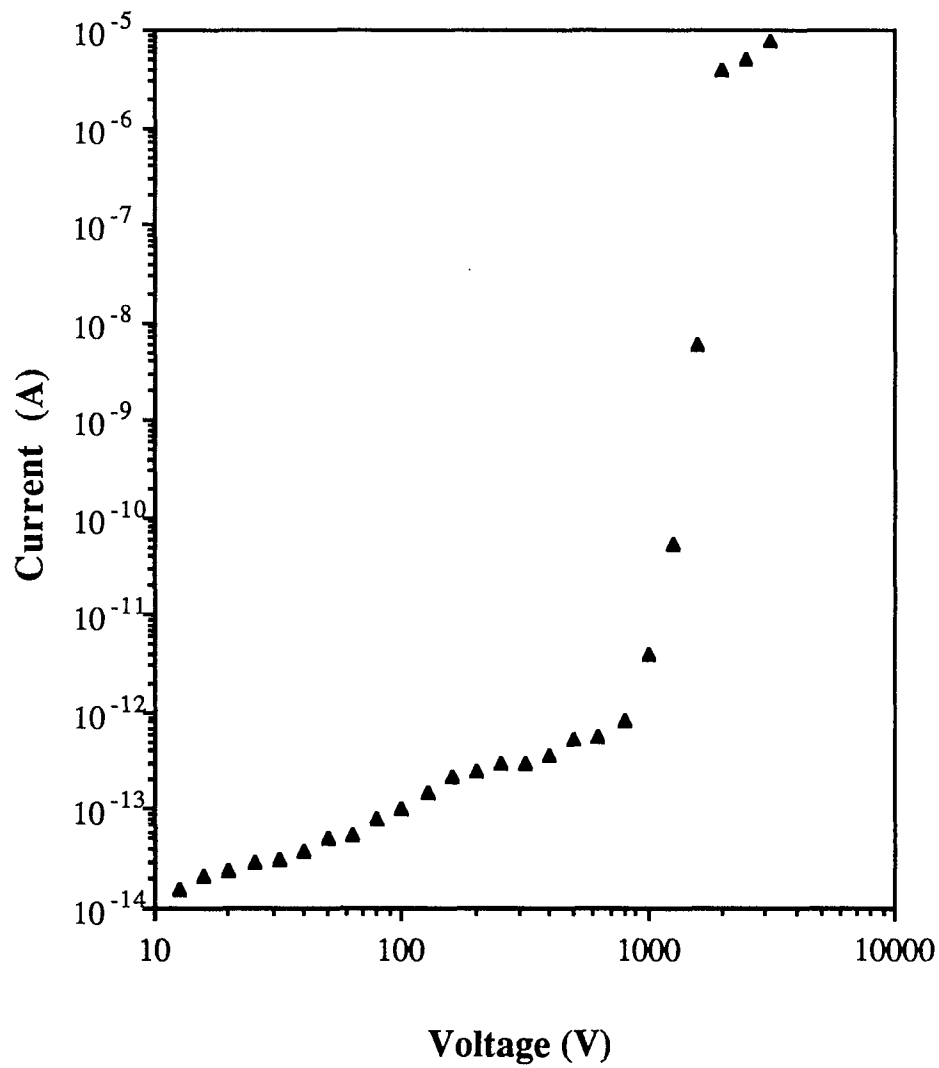
The type Ia diamond used in this investigation was a synthetic diamond produced by the Sumitomo Corporation. The diamond was formed using a high pressure, high temperature anvil process. Because the diamonds were originally intended to be used as heat sinks for semiconductor devices, large amounts of nitrogen is incorporated into the diamond crystals during the growth process. The high concentration of nitrogen increases the thermal conductivity of the diamond and thus increases the heat conduction away from the semiconductor devices.

The nitrogen, in addition to increasing the thermal conductivity, gives the diamond a yellow color when introduced at high concentrations found in heat sink and natural diamonds. The majority of the nitrogen found in synthetic and natural type Ia diamonds does not occupy lattice sites within the crystal but is found in clusters or aggregates [2].

The electrical characteristics of the type Ia diamond were investigated using I-V measurements. Silver epoxy contacts were applied to opposite parallel faces of a synthetic diamond with dimensions $3 \times 3 \times 1.5 \text{ mm}^3$. The contacts were placed on the larger faces and had an area of 1.9 mm^2 and the thickness of the sample was 1.5 mm. The results of the measurement is shown in Graph 1. The voltage was varied from 10 to 3100 V, in order to see the various regions of conduction.

3.2.2 Type IIb Diamond

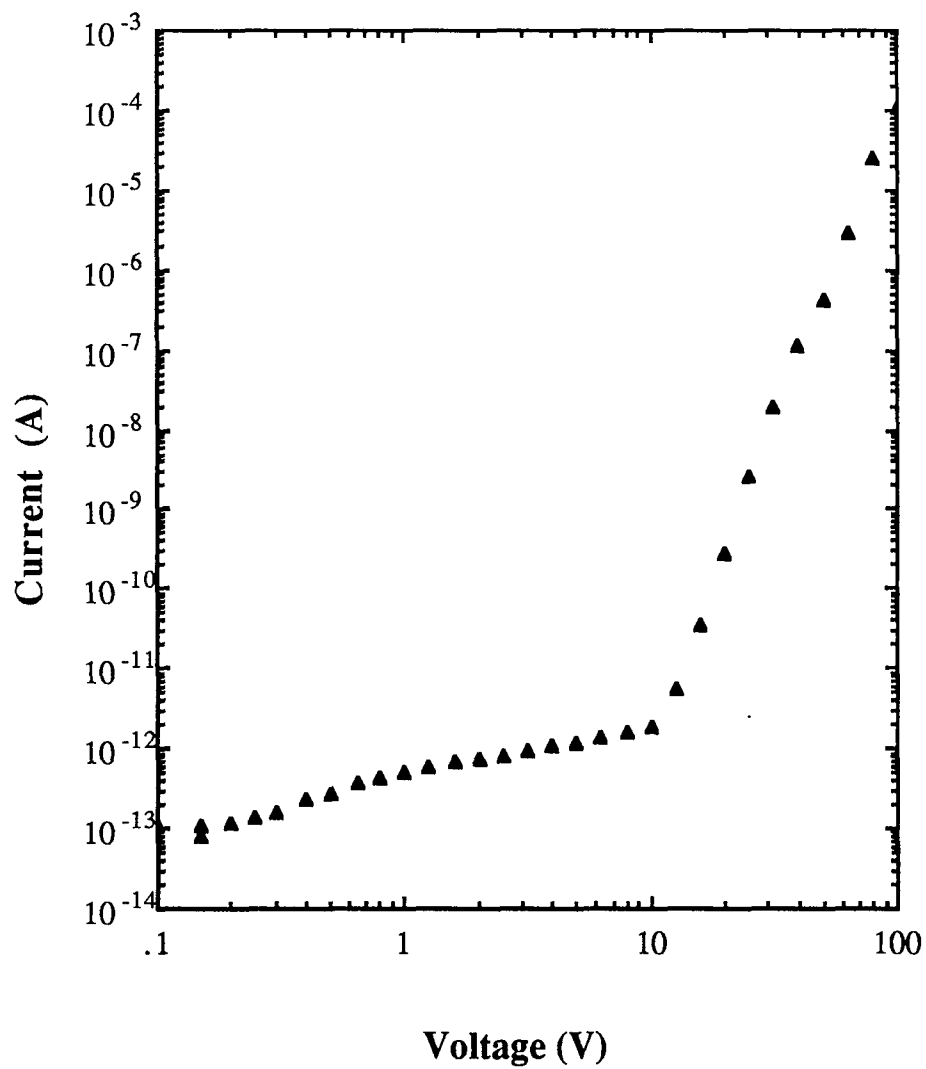
The second diamond investigated in this study was a type IIb semiconducting diamond. Natural semiconducting diamonds such as this one are very rare. Type IIb diamond contains boron atoms in substitutional sites which form a shallow acceptor located 0.368 eV above the valence band. Boron impurities have a significant effect on the conduction in diamond. Natural semiconducting diamond can have resistivities ranging from 10 to greater than $10^{10} \Omega \cdot \text{cm}$, as compared to most other diamonds having resistivities greater than $10^{16} \Omega \cdot \text{cm}$.



Graph 1. I-V characteristics of type Ia diamond

High concentrations of boron can give the diamond a blue color. Natural blue diamonds are the rarest and most valuable type of diamond. These blue diamonds are known as "Premier Overblues".

The samples used in this study were 3x3x0.25 mm in size and transparent in appearance. Silver epoxy contacts, with an area of 1.8 mm², were applied to the opposite faces. The I-V characteristics were measured over the voltage range from 0.1 to 100 V and are given in Graph 2.



Graph 2. I-V characteristics of type IIb diamond

3.3 Discussion

3.3.1 Type Ia Diamond

The type Ia diamond exhibited I-V characteristic similar to that observed in Figure 4b. This is the case of an insulator, or wide bandgap semiconductor, with a single deep trap level. The current changes from linear to trap-filled limit and then to a square law behavior. The trap in this case lies below the Fermi level and is nearly full under thermal equilibrium. As given in equation 3.20, the concentration of traps which are empty is given by

$$p_{t,o} = 2V_{TFL} \epsilon / qL^2,$$

where V_{TFL} is the voltage at which the I-V curve makes its transition from ohmic to TFL, L is the thickness and ϵ is the dielectric constant of the sample. Using the data given in Graph 1, V_{TFL} is 800 V and L is 1.5 mm, yielding an unfilled trap density of $2.2 \times 10^{11} \text{ cm}^{-3}$. Looking at Graph 1, the ratio of $I(V_{TFL})/I(2V_{TFL})$ is approximately three orders of magnitude. Because the ratio of unfilled traps to free carrier density is equal to this ratio of currents, this implies that $p_{t,o}$ is at least three orders of magnitude greater than the free carrier concentration, n_o . The conduction in this sample, therefore, is dominated by the trap. The resistivity for this sample is calculated to be $8 \times 10^{15} \Omega \cdot \text{cm}$, which is within the values given for type Ia diamonds.

3.3.2 Type IIb Diamond

The type IIb diamond sample again showed behavior characteristic of a single deep trap. The resistivity of this sample is $1.4 \times 10^{13} \Omega \cdot \text{cm}$. This is a very high resistance for a semiconductor, however, p-type conductivity was confirmed using the hot probe technique. The number of unfilled traps for this sample using V_{TFL} equal to 11 V and a sample thickness of 0.25 mm is $1.1 \times 10^{11} \text{ cm}^{-3}$. Again, taking the ratio of the current at twice V_{TFL} and the current at V_{TFL} , it is seen that the conduction is dominated by the traps.

Using I-V measurements, information about the unfilled trap density can be determined. Although no information about the trap energy can be determined from I-V measurements, other methods such as photoconductive spectroscopy can be used.

CHAPTER 4

PHOTOCONDUCTIVITY IN SEMICONDUCTORS

4.1 Theory of Photoconductivity

The formation of free charge carriers in a semiconductor requires sufficient energy to overcome the energy gap between valence and conduction bands or between localized impurities and these allowed bands [12]. For temperatures above absolute zero, thermal excitation and ionization takes place within the semiconductor bulk and produces free carriers in the conduction and valence bands. The process of thermal ionization follows the rules of Fermi-Dirac statistics.

Any radiation with an energy greater than the bandgap or with sufficient energy to excite carrier to and from the impurity level can generate free carrier within the semiconductor. Free carriers can be produced when an incident electron beam impinges upon the crystal and ionizes carriers through impact ionization. One application in which this type of ionization is used is electron beam induced current (EBIC) spectroscopy. EBIC is used in semiconductor characterization to determine carrier lifetimes, diffusion lengths and to locate electrically active defects.

Photons can also be used to generate free carriers in the bulk of a semiconductor. The most common type of measurement involving the optical excitation of carriers is photocurrent spectroscopy. In addition to being able to measure the band gap of direct semiconductors, photoconductivity measurements are able to reveal information about impurity levels within the forbidden band.

4.1.1 Fundamental Photoconductivity

In a crystal, electrons interact strongly with the lattice atoms, and thus, assuming no external ionization, the electron and lattice temperatures are nearly identical. By illuminating the semiconductor with photons which have an energy $h\nu > E_g$, the average thermal energy of the electrons is increased through the photoexcitation process while, the lattice temperature remains relatively unaffected. Consequently, the thermal equilibrium between the lattice and the electrons is disturbed. After the light source is removed, the thermal equilibrium between lattice and electrons is re-established through the process of recombination of carriers. The energy given up to the lattice through this recombination process is much smaller than the total thermal energy of the lattice. The temperature of the semiconductor as a whole is left relatively unchanged.

Using the fact that the equilibrium carrier concentration is left unchanged, the total concentration of carriers can be written as the sum of the equilibrium (n_o, p_o) and non-equilibrium ($\Delta n, \Delta p$) carrier densities.

$$\begin{aligned} n &= n_o + \Delta n \\ p &= p_o + \Delta p \end{aligned} \quad (4.1)$$

The presence of these non-equilibrium carriers causes a change in the bulk conductivity. The general conductivity is given by

$$\sigma = q(\mu_n n_o + \mu_p p_o + \mu_n \Delta n + \mu_p \Delta p), \quad (4.2)$$

where μ_n and μ_p are the electron and hole mobilities respectively. The change in conductivity can be written as

$$\Delta\sigma = q(\mu_n \Delta n + \mu_p \Delta p). \quad (4.3)$$

In order to understand photoconductivity, one must know the factors which affect the non-equilibrium carrier concentrations. Assuming a constant absorption coefficient, the optical energy absorbed per unit time per unit volume is given by

$$-\frac{dI}{dx} = \alpha I, \quad (4.4)$$

where I is the intensity of the incident light, α is the optical absorption coefficient, and x is in the direction of propagation.

The number of carriers generated by the light per unit time per unit volume is proportional to αI . Integrating equation (4.4) with respect to time yields the carrier concentration

$$\Delta n = \Delta p = \beta \alpha I t \quad , \quad (4.5)$$

where β is the constant of proportionality. These carrier concentration values neglect the effects of recombination. If recombination is taken into account, the change in carrier concentration saturates at a value of

$$\begin{aligned} \Delta n_{ss} &= \beta \alpha I \tau_n \quad \text{and} \\ \Delta p_{ss} &= \beta \alpha I \tau_p \quad , \end{aligned} \quad (4.6)$$

where the steady state values, denoted by ss, depend on the electron and hole recombination lifetimes, τ_n and τ_p respectively.

Given the value for the excess carrier densities, the steady state change in conductivity is given by

$$\Delta \sigma_{ss} = q \beta \alpha I (\mu_n \tau_n + \mu_p \tau_p). \quad (4.7)$$

Because the mobility lifetime product $\mu_n \tau_n$ is greater than $\mu_p \tau_p$, the photoconductivity, governed by equation 4.7, is typically unipolar. The non-equilibrium conductivity can be written as

$$\Delta \sigma_{ss} = q \beta \alpha I \mu \tau. \quad (4.8)$$

4.1.2 Impurity Photoconductivity

Up to this point, only fundamental photoconductivity using photons with an energy greater than the bandgap to excite carriers has been considered. Using this type of photoconductive measurement, information about the effects of recombination levels on the lifetimes of the carrier can be found; but no details of the position of the level within the

band structure can be obtained. Impurity photoconductivity uses radiation which has an energy smaller than the band gap to probe the various impurity or defect levels which may exist within the semiconductor.

Figure 6 shows a typical band structure of a semiconductor and its corresponding photoconductive spectra. In Figure 6a, there are three wavelengths at which the semiconductor will absorb the light and generate free carriers. The first wavelength, which is the shortest, is the fundamental absorption. This corresponds to a direct generation of electron hole pairs and was discussed in the previous section. On the photoconductive spectra, Figure 6b, this fundamental absorption region is to the left of the graph and extends down to a wavelength at which the electrons are excited beyond the conduction band width. A second type of excitation occurs by exciting electrons out of the trap and into the conduction band. In this process, a conduction electron is generated with no corresponding hole. The rate of trapped electron excitation is much smaller than that of bandgap excitation, due to the small population of electrons found in the traps as compared with the number of electrons in the valence band. The corresponding change in conductivity induced by this second wavelength of light will be much smaller than that seen in band edge excitations. The third type of excitation is one in which a valence band electron is excited into the trap level. This generates a hole in the valence band and thus adds to the conductivity. The rate of generation for excitation into a trap is less than fundamental photoconductivity due to the limited number of terminal states in the trap level.

In addition to these direct generation processes, as electrons are excited to the traps or excited out of the traps, the number of empty traps changes. Because photoconductive measurements are made while the sample is biased at some injection level, the rate at which the injected carriers are trapped is also affected. If the incident light is tuned such that the traps are completely filled, then the current density and the conductivity will increase because, no further injected carriers can be trapped. All of the injected carriers will be free and will increase the conduction current.

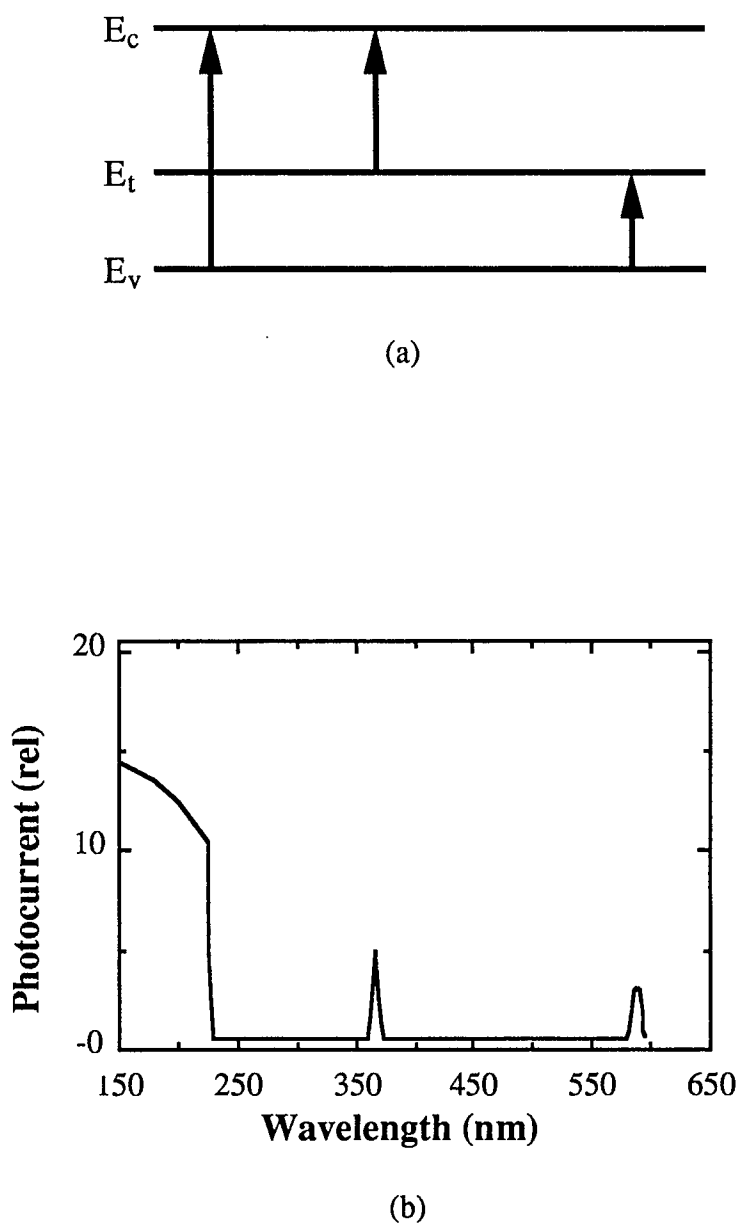


Figure 6. Photoconductivity in a Semiconductor (a) Band Structure and (b) Photoconductive Spectrum

An additional effect of exciting electrons to or from a trap level is that the thermal equilibrium of carriers between the levels can be altered. As an example, if the incident light is tuned to excite the electrons from the impurity level to the conduction band, as seen in Figure 6a, the reduction in electron density of the impurity level, may disturb the thermal equilibrium between these levels and the valence band. As a result of the new thermal equilibrium, the hole concentration in the valence band may increase. In this respect, radiation which started out producing only electron carriers also generated holes.

One important difference between fundamental and impurity photoconductivities is that while the former is linearly dependent on the incident light intensity, impurity photoconductivity is will at higher optical flux densities. The reason behind this is the relationship between the conductivity and the local absorption coefficient. In general, the probability of photon absorption and the corresponding electron transition is proportional to the electron density in the initial state and the hole density or number of empty states in the final level. In the case of fundamental photoconductivity, the levels involved are the valence and conduction bands. Even illumination with light of the highest possible intensity is unable to alter the electron density in the valence band and the density of holes in the conduction band. As a result, the absorption coefficient of this transition is independent of the light intensity.

The situation is different for impurity photoconductivity. If the excitation source is tuned such that electrons are being excited from the valence band into the trap and thus producing holes, even at moderate light intensities, the number of empty states in the trap approaches zero rapidly and thus reduces the absorption coefficient. Since the rate of generation of carriers is $\beta\alpha I$ and the absorption coefficient is not constant, the corresponding change in conductivity is no longer linearly dependent upon the light intensity but takes on some other dependence [12].

4.2 Experimental Results

In order to further understand the conduction mechanisms in diamond samples with traps, trap energy and concentration must be determined. Spectroscopic photoconductivity measurements can be used. By studying the changes in photo-induced currents while varying the wavelength of incident light, the trap levels can be identified.

The system used in this study included a broadband light source, a monochromator, a sample chamber, an electrometer, and a computer for system control. A system diagram is shown in Figure 7. The light is generated by a Xenon arc lamp which generates 150 W of radiant energy. The light is collected and collimated by several lenses. This broadband light is passed through a monochromator and split into its spectral components. The output of the monochromator is divided into two beams using a beamsplitter, one of which is sent to a photomultiplier tube (PMT) for normalization. The output of the PMT is sent to a computer. In order to remove the effects of source fluctuations, the raw photoconductivity spectrum is divided by this PMT normalization signal. The sample, which is under an electrical bias, is illuminated with the second beam of monochromatic light. The photocurrent is then determined by measuring the sample current while under illumination and subtracting the dark current at the same bias. As in the I-V measurements, the current is sampled 20 times and averaged to minimize fluctuations.

After the data point for a specific wavelength is determined, the wavelength of the monochromator is stepped and the measurement repeated. The system is capable of covering the wavelength range from 400 to 825 nm, which corresponds to an energy range of 1.5 to 3.1 eV. The spectral output of the Xe lamp, which was used for normalization of the photoconductivity measurements, is shown in Graph 3. In order to extend this range, a source with more energy in the infrared must be used and the PMT must be replaced with a semiconductor detector. For this study, however, the original spectral range was found to be sufficient.

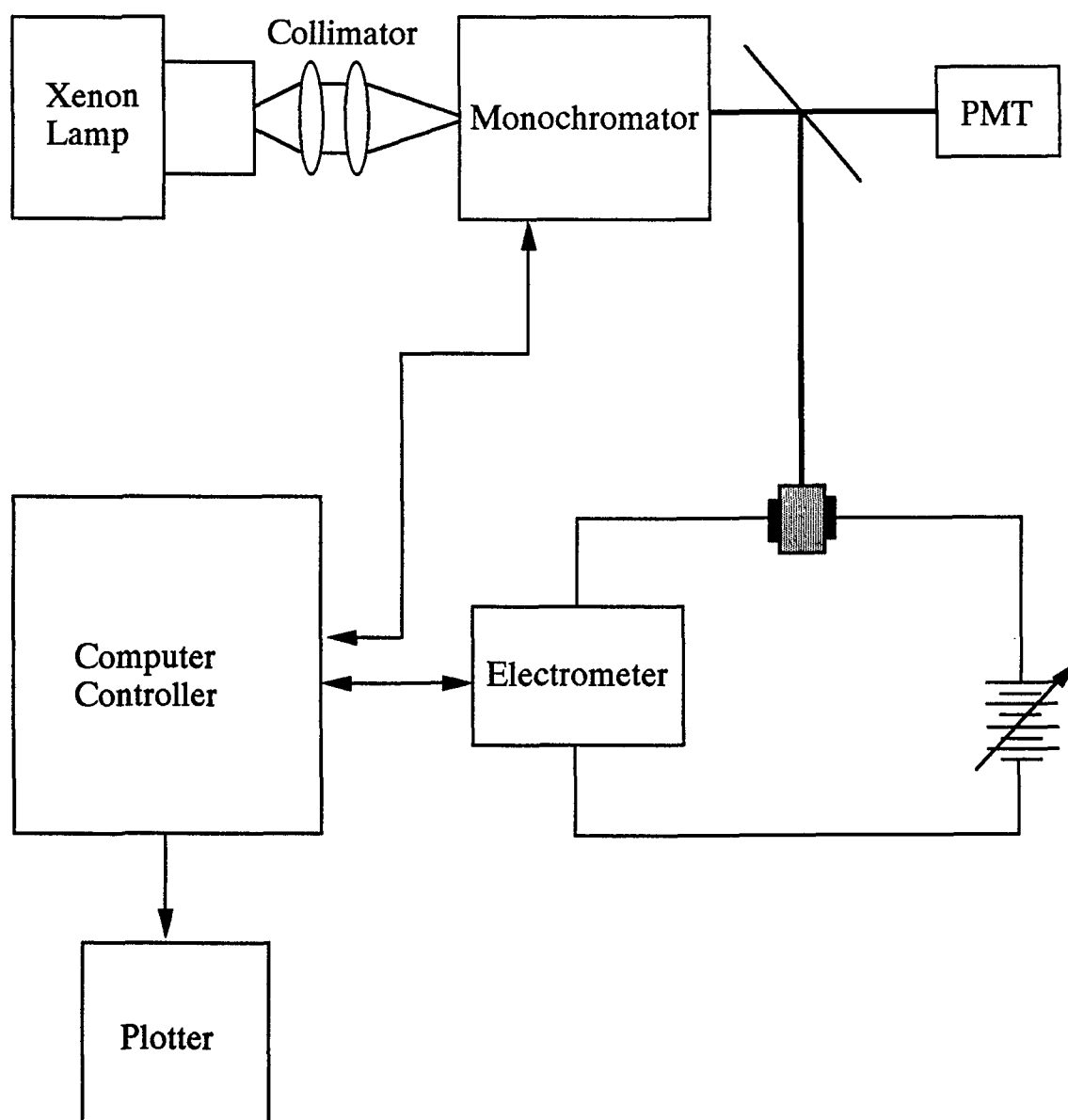
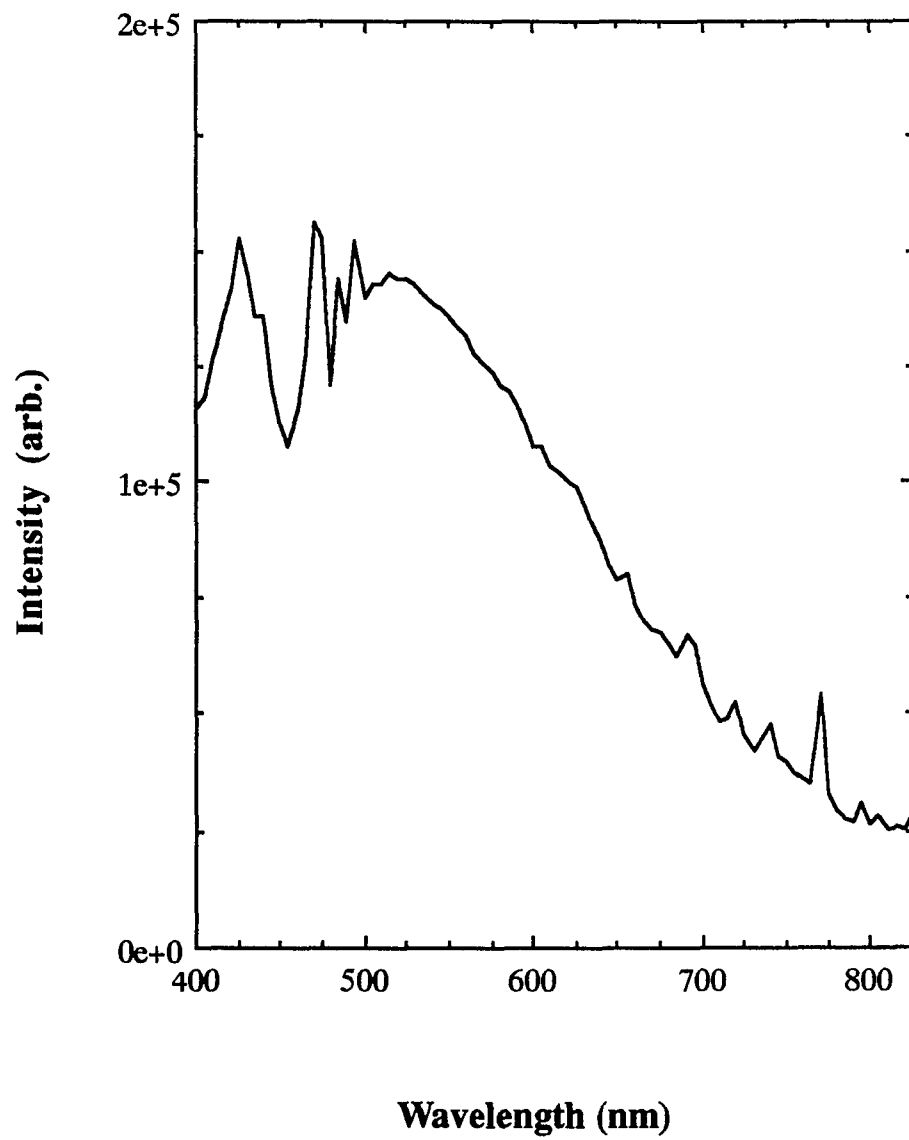


Figure 7. Photoconductivity Measurement System



Graph 3. Emission spectrum for xenon arc lamp

4.2.1 Type Ia Diamond

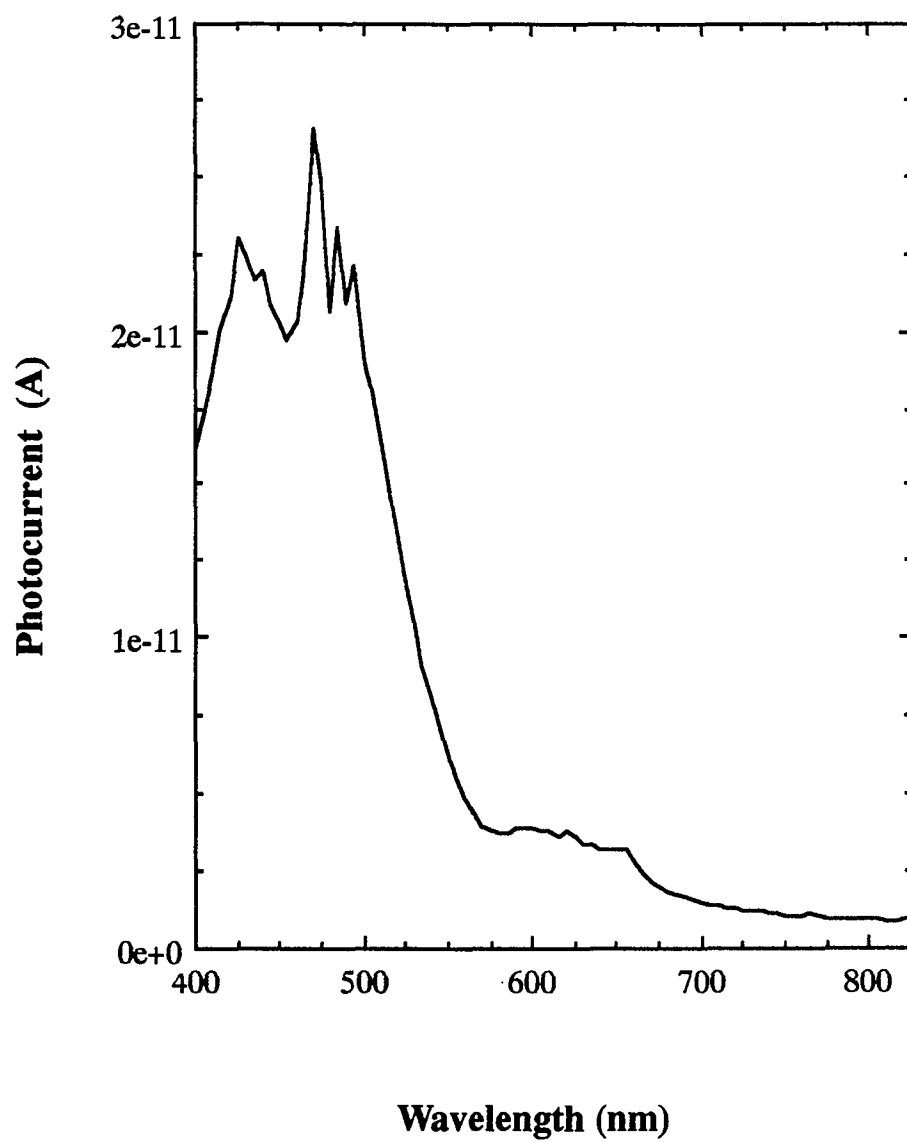
The type Ia diamond was biased at the highest voltage setting provided by the internal voltage source of the Keithley electrometer, 100V, because of its high resistance, 10^{13} ohms, . The results of the photoconductivity measurement are given in Graphs 4 and 5. Graph 4 shows the raw photoconductive spectrum prior to subtraction of the dark current and normalization due to the fluctuations of the light source. After correcting the spectrum, the corrected photoconductivity spectrum is given in Graph 5. The measurements were made over the spectral range of the system, 400 to 825 nm.

4.2.2 Type IIb Diamond

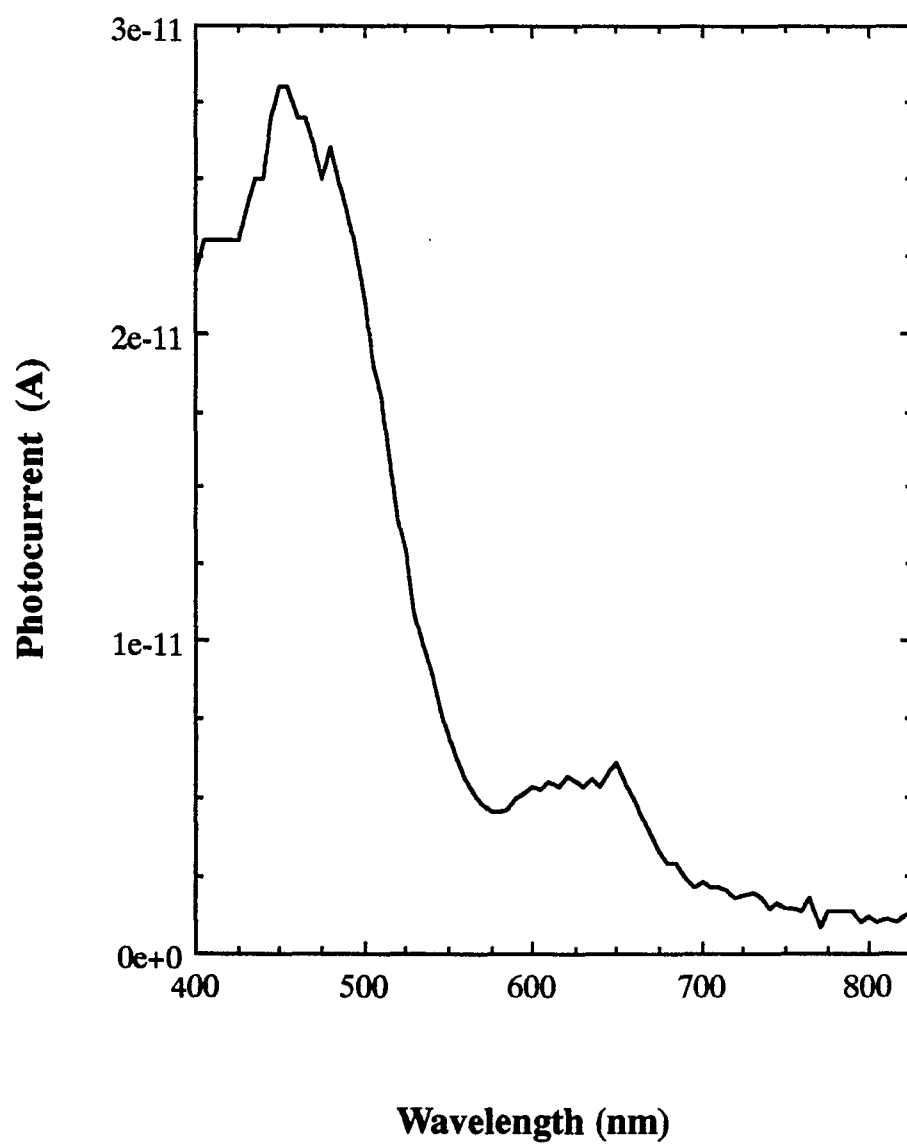
The photoconductivity of the type IIb semiconducting diamond was measured at several bias conditions. It was found that measurements made at high injection levels desensitized the system. Because the number of optically generated carriers is relatively independent of injection level, and therefore, the increase in conductivity remains constant for a fixed light intensity. The measured signal is proportional to the sum of the injected and the optically generated charges. At high injection levels, the optically generated component of the conductivity, or photoconductivity, becomes a very small percent of the measured signal, and therefore, cannot be accurately determined.

When the sample was biased in the trap filled limit region, or nearly vertical region of the I-V curve, small fluctuations in the voltage source were amplified to substantial current changes. This made photoconductivity measurements in this region extremely noisy.

The spectrum was recorded by biasing the sample in the most sensitive ohmic region. For the type IIb diamond this region extended from 0.1 to 10 V. The bias was chosen small enough to minimize the signal due to the thermal free carriers, but large



Graph 4. Uncorrected photoconductivity spectrum for type Ia diamond



Graph 5. Corrected photoconductivity spectrum for type Ia diamond

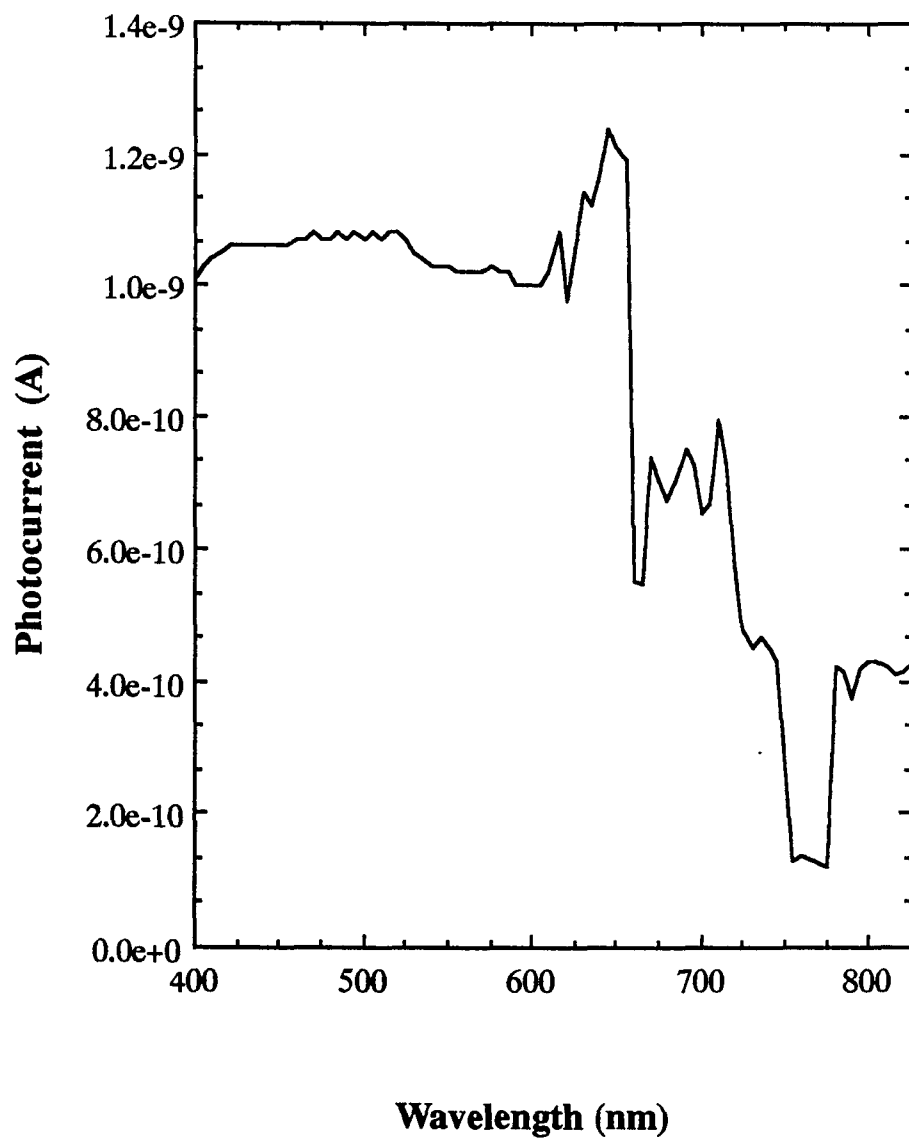
enough to provide a sufficiently stable current. The voltage chosen for this sample was 0.5 V. The uncorrected and corrected photoconductive spectra are given in Graphs 6 and 7, respectively. The measurement was again made over the complete spectral range of the system.

4.3 Discussion

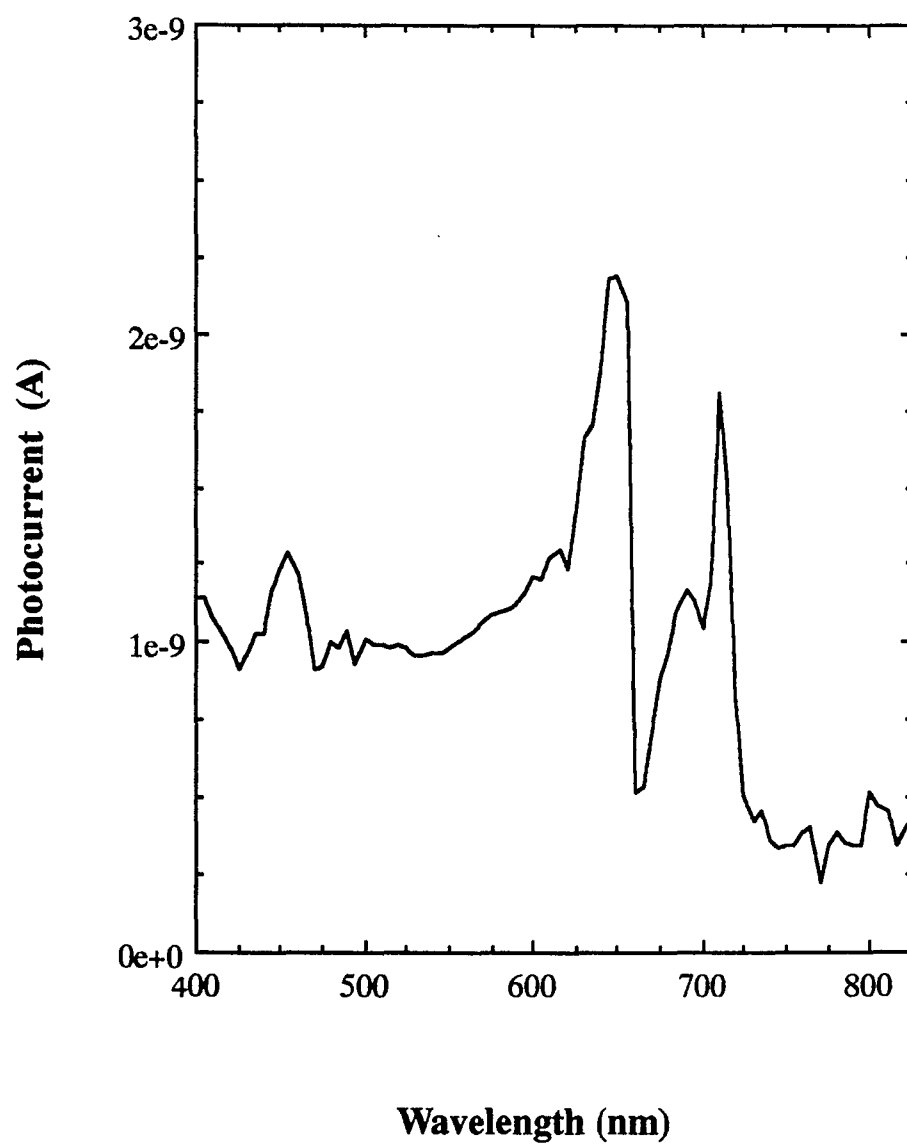
The photoconductivity measurements for both samples were made with radiation ranging in energy from the bandgap of diamond divided by two, 2.73 out to 1.5 eV. Because the traps in both samples were located below the Fermi level, this range of energy should identify the trap levels provided they are not too close to the valence band. The deep levels were probed by exciting an electron from the valence band to the trap level.

4.3.1 Type Ia Diamond

The photoconductivity measurement for the type Ia sample revealed the presence of two peaks. The largest of these was centered about 455 nm, or 2.725 eV. The bandgap of diamond is 5.46 eV [2], which places this primary photoconductive peak at the middle of the forbidden band. Recalling the results from the I-V measurements, the trap level was found to be deep and thus below the Fermi level. This seems to indicate a contradiction. How can a trap exist at precisely the intrinsic Fermi level and be a deep trap, one which is at least kT below the Fermi level. One possible solution to this dilemma is that the primary photoconductive peak may be the convolution of two peaks. To explain this, the trap level is placed $2kT$ below midgap. With a photon energy of 2.67 eV, corresponding to a wavelength of 464 nm, electrons will be excited from the valence band to the trap. In addition, electrons could be excited from the trap to the conduction band, also giving rise to an increase in conductivity. This second excitation would require photons with an energy of 2.79 eV or 444 nm. The convolution of the two peaks might appear as one on the current system due to a limited spectral resolution of 5 nm. This leads to the conclusion



Graph 6. Uncorrected photoconductivity spectrum for type IIb diamond



Graph 7. Corrected photoconductivity spectrum for type IIb diamond

that the primary trap level is located 2.7 eV above the valence band, plus or minus a few kT .

A second photoconductivity peak, as seen in Graph 5, is located at 630 nm or 1.96 eV. This peak has a smaller amplitude than the primary peak. This indicates that either the photon excitation cross section is smaller or the density of empty states in the trap is less than the previous case. Since the density of unfilled traps behaves according to Fermi statistics, one would expect that since the second trap was further below the Fermi level, the density of unoccupied traps would be smaller. The absolute densities of the two trap cannot be determined due to the lack of information on the position of the Fermi level.

4.3.2 Type IIb Diamond

The photoconductivity spectrum, as seen in Graph 7, shows two peaks. The first of these is located at 640 nm or 1.94 eV above the valence band. The position is measured with respect to the valence band due to the fact that the trap was earlier identified as being below the Fermi level. The second trap is located at 710 nm, or 1.75 eV above the valence band. As before, the densities of the two traps cannot be determined because the position of the Fermi level is not known.

CHAPTER 5

EFFECTS OF HYDROGENATION IN DIAMOND

5.1 Effects of Hydrogenation in Semiconductors

In recent years, the study of hydrogenation of semiconductors has become important because the electrical and optical properties of these materials are altered by the presence of hydrogen. In the case of Si, atomic hydrogen reduces the leakage current of pn junctions [13] and neutralizes boron acceptors [14-16] and shallow donors [17]. In addition, hydrogen has been found to passivate point defects and neutralize deep level defects in Si due to Au, Cu and Ni [18-20]. Grain boundary passivation in poly-Si is also reported [21-23]. Similarly, Cu related defects in Ge are passivated by atomic hydrogen [24]. Changes in the electrical and optical characteristics of amorphous Si have been observed [25]. Hydrogen passivation effects are also observed in III-V compounds. Acceptors in InP, in addition to being passivated [26], also impede the diffusion of hydrogen. Photoluminescence intensities of III-V compound have been observed to increase up to four orders of magnitude [27]. In view of these results, hydrogen has been proposed as a passivation agent for defects in polycrystalline superlattices and quantum wells [28]. Similar effects are expected in diamond, which will be useful for electronic devices.

Hydrogen passivation of deep donors has been suggested and the increase in conductivity is thought to be due to shallow acceptor levels. Atomic hydrogen alters the electronic and optical properties of semiconductors. Using current-voltage measurements, it has been shown that not only can the changes in conduction due to the introduction of

hydrogen be measured but the amount of electrically active hydrogen can be quantified [29].

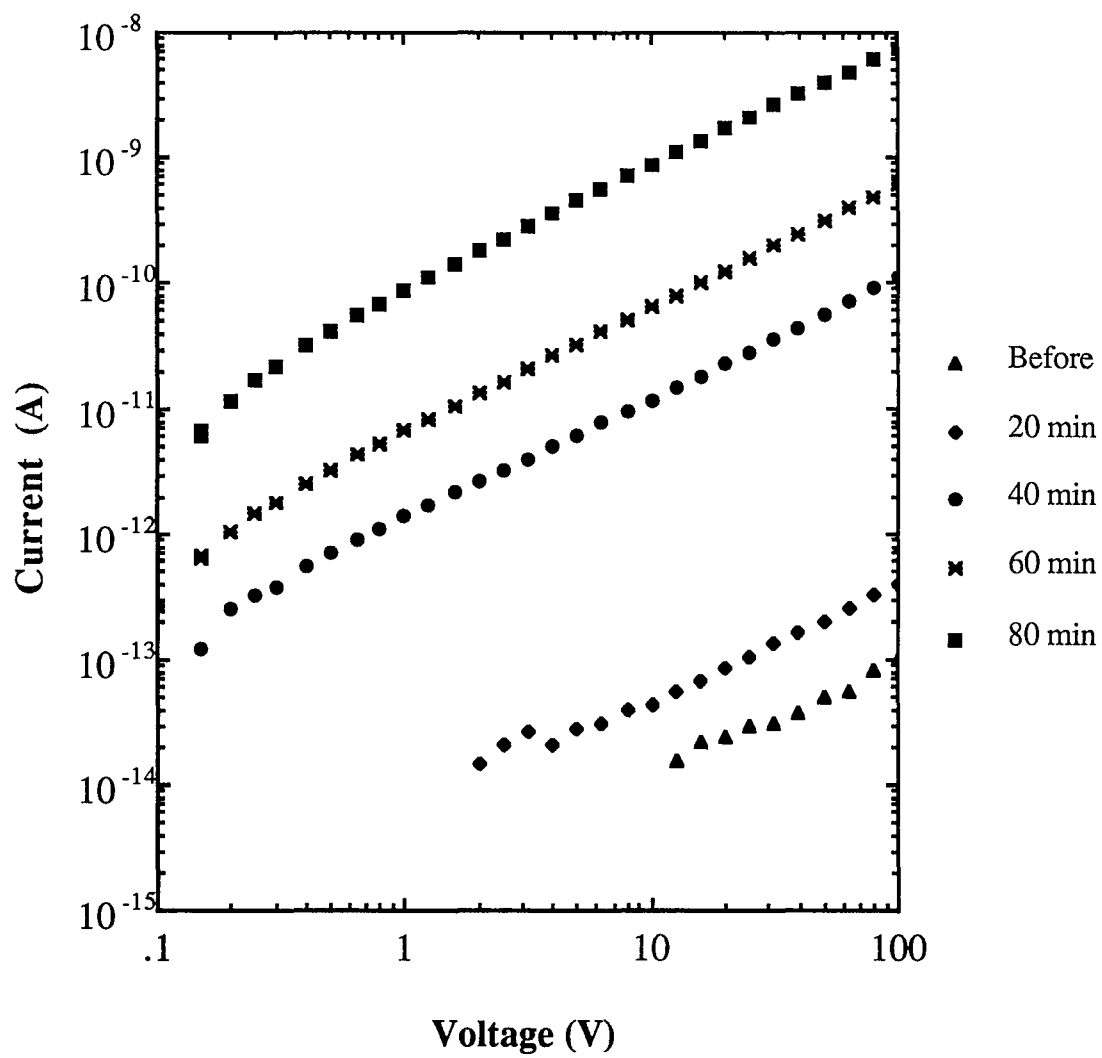
5.2 Experimental Results

In order to hydrogenate the diamond samples, they must be exposed to atomic hydrogen. The simplest method of generating atomic hydrogen is using a plasma discharge. Two plasma systems were used for the purpose of hydrogenation. The first system was a capacitively coupled barrel plasma system with an rf (13.56 MHz) power source. The second system was a microwave plasma system. The microwave system had the option to externally control the temperature of the substrate using induction heating. It provided greater control over the hydrogenation process.

Prior to the start of hydrogenation, the diamond samples were annealed in a vacuum at 700° C for 4 hours. The annealing removed all traces of hydrogen from the diamonds. After annealing, the I-V characteristics were measured in order to determine the initial conditions. The samples were then exposed to the hydrogen plasma for 20 minutes and the I-V measurements were repeated. The diamonds were again placed in the plasma for 20 minutes, giving a cumulative 40 minute exposure. The samples were cycled between the plasma and I-V systems in order to determine the systematic changes in conduction.

5.2.1 Type Ia Diamond

The type Ia diamond was first hydrogenated in the rf plasma system. The plasma conditions were 500 mTorr of hydrogen at 10 sccm of flow. The results for the unhydrogenated sample and 20, 40, 60, and 80 minutes of hydrogenation are shown in Graph 8. The sample temperature, although not externally controlled, was measured at 105° C for a 50 watt plasma. The heat required to raise the temperature was provided by the plasma and the temperature reached this steady state value after five minutes of operation.



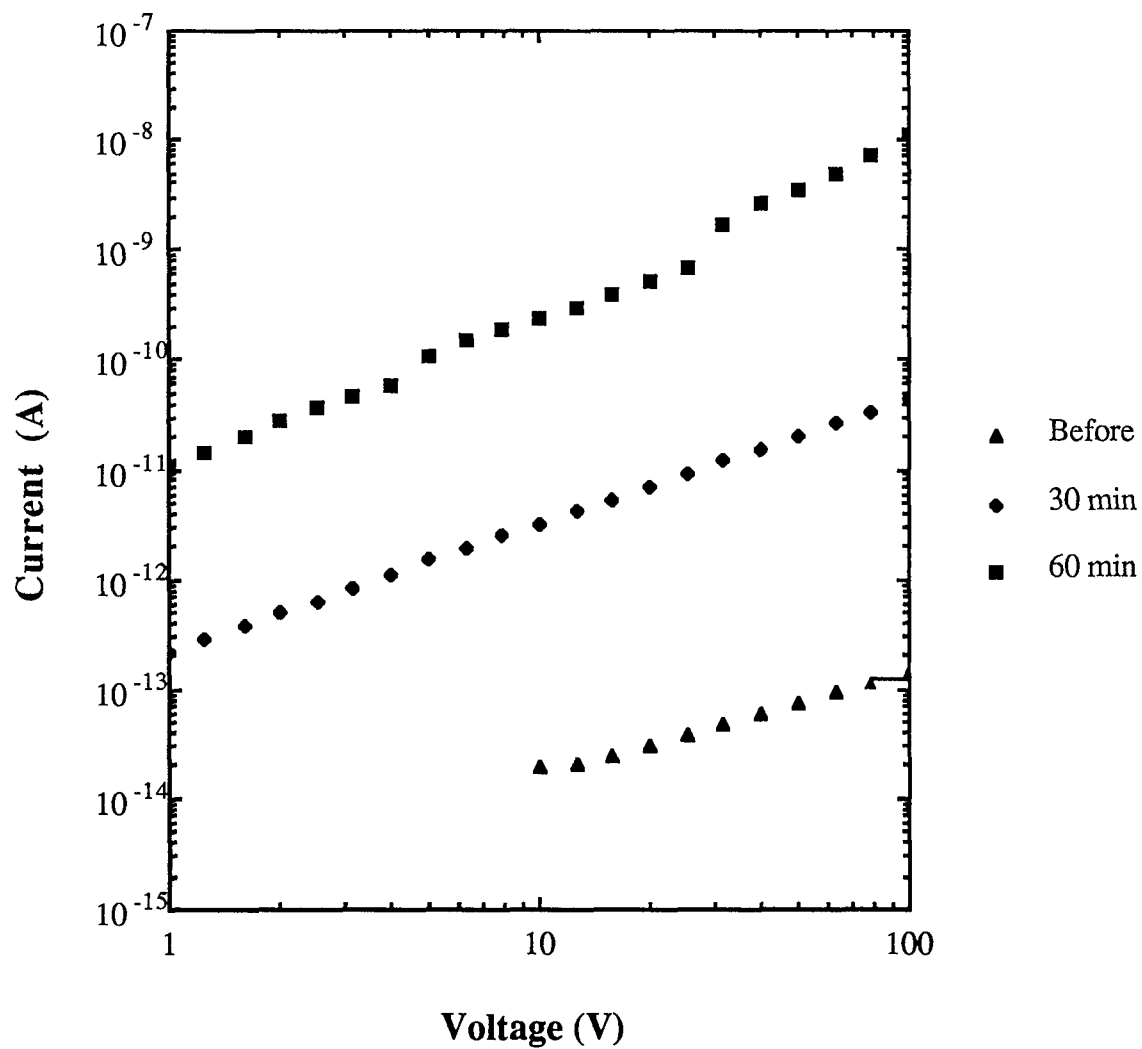
Graph 8. I-V characteristics of type Ia diamond hydrogenated in rf plasma

The sample was then annealed back to its original state and then exposed to the microwave generated plasma. The plasma was operated at 10 Torr and 500 sccm of hydrogen and 750 watts of 2.45 GHz radiation. The temperature of the sample was set at 200° C, which was the minimum temperature for stable operation. The results for 30 and 60 minutes of hydrogenation are shown in Graph 9.

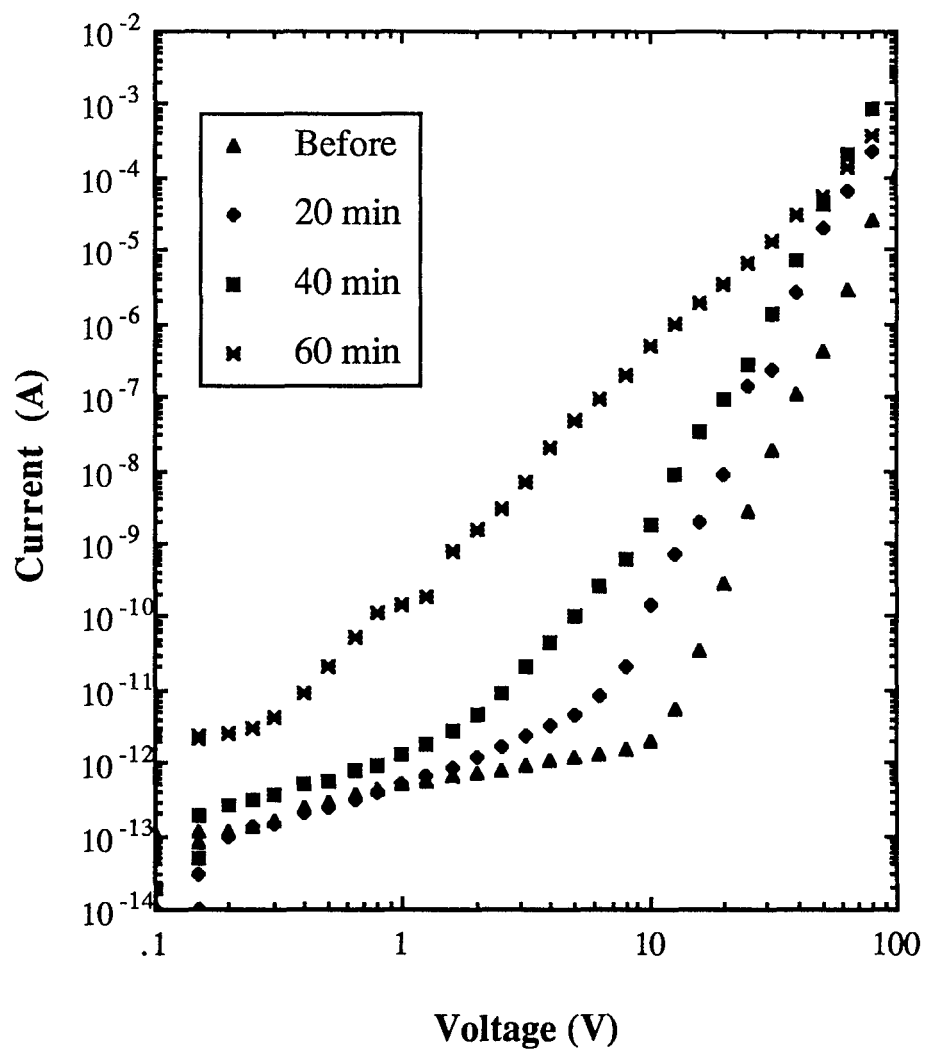
One problem encountered during the hydrogenation of the type Ia sample was that when the voltage applied to the sample during the I-V measurement was taken above 100 V, the shifts in current due to hydrogenation would disappear. The I-V shifted back to the unhydrogenated values. As long as the sample was not biased at high voltages, the hydrogenation had a cumulative effect and continued to increase the sample conductivity. This may be due to the hydrogen drifting in high fields and depleting a region of the sample, thus increasing the overall resistivity. Because of this problem, the type Ia sample could not be characterized beyond the ohmic region of conduction.

5.2.2 Type IIb Diamond

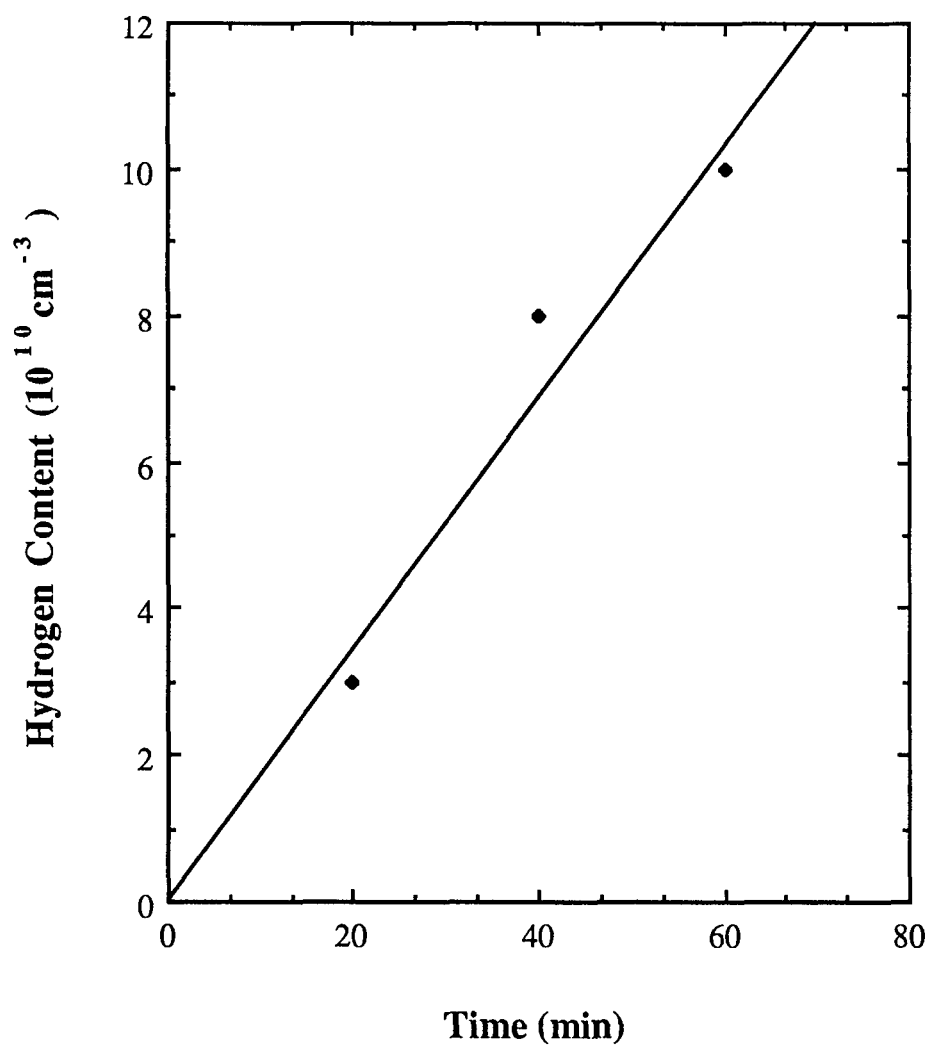
The semiconducting diamonds, when hydrogenated, yielded the most interesting results of this study. The type IIb samples were hydrogenated in the microwave plasma system under the same conditions as used for the type Ia sample. The results of hydrogenation for 20, 40 and 60 minutes are given in Graph 10. The increases in conductivity continued beyond the first hour and so the hydrogenation was continued in order to determine the saturation point if any existed. The shift in the I-V after four hours is shown in Graph 11. After this point no further increase in conductivity was observed.



Graph 9. I-V characteristics of type Ia diamond hydrogenated in microwave plasma



Graph 10. I-V characteristics of type IIb diamond hydrogenated in microwave plasma



Graph 11. Hydrogen content versus time

5.3 Discussion

5.3.1 Type Ia Diamond

The conductivity of the type Ia diamond increased by five order of magnitude following hydrogenation for 80 and 60 minutes for the rf and microwave systems respectively. The plasma density of the microwave system was several orders of magnitude higher than that of the rf system. This was due to the higher gas pressure, higher power deposition and higher efficiency of the microwave system. Even though the plasma densities varied so significantly, the shifts of the I-V curves were approximately equal.

The small differences in hydrogenation rate can be explained by the diffusion rate of hydrogen in diamond. While the diamond in the microwave system was exposed to the hydrogen plasma, its temperature was 473° K. The temperature of operation in the rf system was only 378° K. If the current increase is proportional to the number of diffused hydrogen atoms and the diffusion rate is proportional to the temperature, then the variation in the current increase for a given time can be accounted for by the increase in temperature. This leads to the conclusion that the hydrogenation is independent of plasma density and only dependent on the diamond temperature. Hydrogenation is, therefore, a diffusion limited process. By increasing the temperature of hydrogenation the rate should also increase.

5.3.2 Type IIb Diamond

The type IIb diamond was only exposed to the microwave plasma due to the independence of hydrogenation and plasma density, and the higher control the microwave system afforded over such variables as temperature. As can be seen in Graph 10, upon hydrogenation the current increases many order of magnitude. In addition to this increase in current, the transition voltage from ohmic to TFL decreases. The transition voltage,

V_{TFL} is proportional to the unfilled trap density as given by equation (3.20). As the diamond is hydrogenated, the traps are compensated. This decrease in trap density is accompanied by a shift of the quasi-Fermi level, F , toward the trap-free Fermi level F_0 . This can be seen in Figure 8, where E_t is the trap level. The unfilled trap concentration is given by

$$p_{t,0} \propto \exp[(E_t - F)/kT] \quad (5.1)$$

As the traps are compensated, F will shift up toward F_0 . This will make $(E_t - F)/kT$ more negative and hence V_{TFL} decreases. From the shift in V_{TFL} on hydrogenation, the amount of electrically active hydrogen introduced in the diamond can be determined. The amount of hydrogen introduced is plotted versus time of hydrogenation in Graph 12. For the limited data, the hydrogenation depends linearly on time. As time is increased, one can hypothesize that the hydrogenation saturates. The rate of hydrogen moving into the sample becomes equal to the out-diffusion rate.

Another feature of the I-V data for the type IIb diamond, is that as the hydrogenation is continued, the slope of the curve in the TFL region decreases. When all of the traps are compensated by hydrogen, the diamond should behave as a trap free crystal. The TFL region will disappear and the I-V will exhibit a transition from ohmic to trap-free square-law regions. The slope changes seen in Graph 10 correspond to this type of transition, for a sample fully hydrogenated.

Upon hydrogenation for four hours, the type IIb sample completely saturated. No further increases in conductivity were seen with addition hydrogenation time. The corresponding I-V is shown in Graph 11. As seen the current makes a transition from ohmic to square-law regions. The traps within the diamond were completely compensated. The current increase due to hydrogenation, was over ten orders of magnitude. This indicates the significance of hydrogenation on trap related conduction mechanisms in a

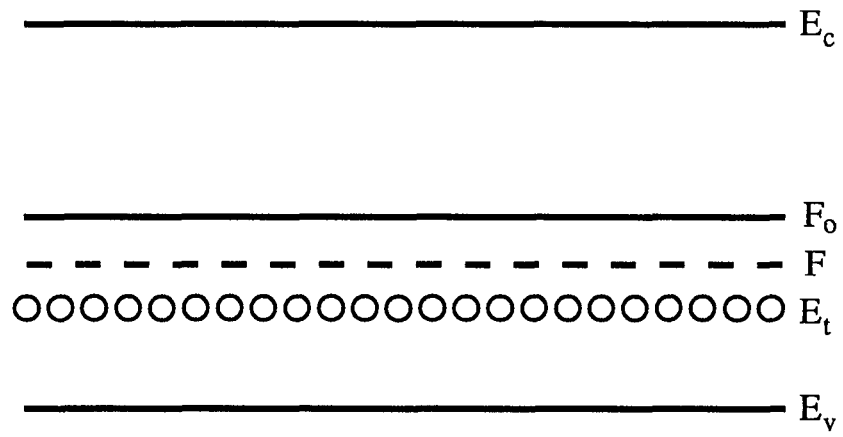
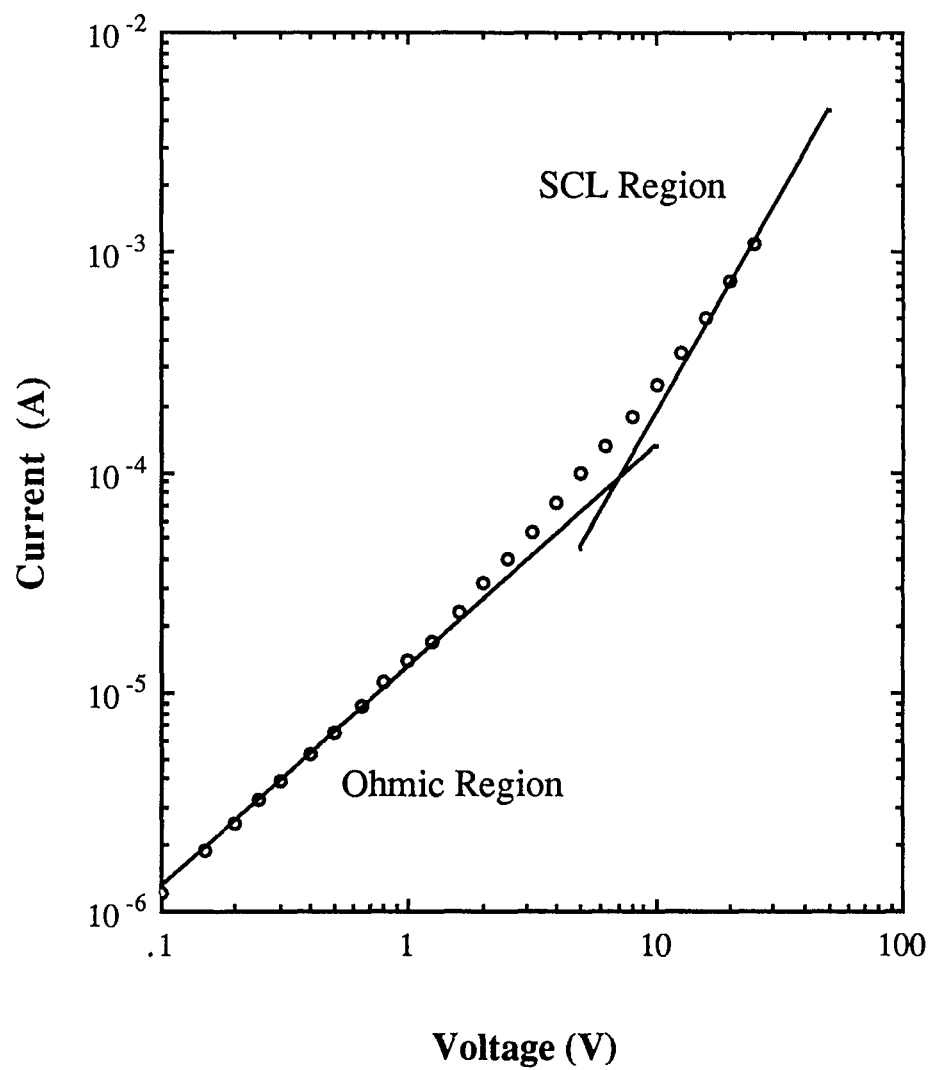


Figure 8. Band Diagram for a Semiconductor Containing a Deep Trap



Graph 12. I-V characteristics of type IIb diamond after four hours of hydrogenation

wide bandgap material like diamond. In a direct band material, this means that the deleterious effects of traps can be eliminated. Hence, it is not surprising to observe the increased photoluminescence efficiency in III-V compounds upon hydrogenation [27].

CHAPTER 6

SUMMARY AND CONCLUSIONS

6.1 Current-Voltage Characteristics of Diamond

The current-voltage measurements proved to be a powerful tool in investigating the conduction mechanisms in diamond. Information on unfilled trap densities could be obtained by careful analysis of the I-V characteristics. The type Ia and IIb diamonds had values of $p_{t,0}$ in the range of 1 to $2 \times 10^{11} \text{ cm}^{-3}$. Using the electrometer system, diamonds with resistivities as high as $10^{16} \Omega \cdot \text{cm}$ could be accurately probed. The resistivities of the two samples were 8×10^{15} and $1.4 \times 10^{13} \Omega \cdot \text{cm}$.

Both types of samples were characterized as containing deep traps. The concentration of traps was several orders of magnitude larger than the free carrier concentration and thus the conduction was dominated by the traps.

6.2 Photoconductivity of Diamond

In order to determine the position of the traps spectroscopic photoconductivity measurements were made. The measurements covered a spectral range from 400 to 825 nm. This range allowed the lower half of the forbidden band to be probed for the presence of traps. Electrons were excited from the valence band into the trap level and thus induced a change in the conductivity.

From the photoconductivity spectrum, it was found that the type Ia diamond contained two traps located at 2.70 and 1.96 eV above the valence band. The relative concentration of the two traps cannot be determined from this measurement as the position

of the Fermi level is unknown. The type IIb sample also contained two trap located at 1.94 and 1.75 eV. Again the total trap concentrations remain unknown.

The I-V measurements showed the presence of only one trap, whereas photoconductivity measurements revealed two. This discrepancy may be due to the difference in trap density. The current characteristic is determined by the trap with the highest concentration, while photoconductivity measurements will reveal all the traps.

6.3 Hydrogenation Effects in Diamond

Hydrogenation of diamond produced a significant increase in conductivity. The type Ia diamond showed an increase of five orders of magnitude, while the type IIb sample showed a maximum shift of ten orders. In addition to increasing the current in the ohmic region, type IIb diamonds showed a shift in the transition from ohmic to trap filled limit regions toward lower voltages. Using the shift in V_{TFL} , the amount of electrically active hydrogen which diffused into the diamond during hydrogenation can be determined. The slope of the TFL region also decreased with increasing hydrogenation time. It was also shown that as the traps were completely compensated by the hydrogen, the I-V no longer contained a TFL region but instead made the transition from ohmic to a trap-free square-law region. This occurred after four hours of hydrogenation. Finally, the hydrogenation process was shown to be independent of the plasma density and it depends only on the diffusivity of the hydrogen in the diamond samples.

When an intentional change in the resistivity of diamond is required for semiconductor devices, hydrogenation can increase the conductivity by several orders of magnitude. In many cases, diamonds are used as heat sinks as well as electrical isolation for semiconductor lasers. The presence of atomic hydrogen can destroy the insulating properties of diamond, hence appropriate caution should be observed to control the operating environment.

6.4 Future Research

One problem encountered, was the inability to resolve photoconductivity change when large dark currents were present. The sensitivity of the systems dropped off sharply once the bias current reached 10^{-11} A. One way to overcome this problem, is to modulate the light intensity. Using a lock-in amplifier, the modulated photoconductivity signal can be resolved regardless of the DC offset. Another possible solution is to use a compensating circuit in order to offset the large dark currents. Both of these techniques would allow the diamond to be probed at higher current levels. Photoconductivity measurements could then be made after hydrogenation, in order to determine the role hydrogen plays in trapping.

Other measurements, such as photoluminescence and absorption, could be made in order to further understand the band structure. In addition, Hall measurements could be used to determine mobilities before and after hydrogenation.

REFERENCES

1. R. Berman and J.C.F. Brock, Proceedings of the Royal Society of London, A289, 46-65, (1965).
2. J.E. Field, "The Properties of Diamond," Academic Press:New York, (1979), p. 14.
3. S. Albin, A. D. Cropper, L. C. Watkins, C. E. Byvik and A. M. Buoncristiani, Optical Engineering, 28, 281-285, (1989).
4. J.F.H. Custers, Physica, 18, 489-496, (1952).
5. C. Canali, E. Gatti and S.F. Kozlov, Nuclear Instruments and Methods, 160, 73-77, (1979).
6. E.M. Omeljanovsky, A.V. Pakhomov and A.Y. Polyakov, Journal of Electronic Materials, 18, 659, (1989).
7. E.H. Rhoderick, "Metal-Semiconductor Contacts," Clarendon Press:Oxford, (1978), p.18.
8. J. Bardeen, Physical Reviews, 71, 717, (1947).
9. P.S. Panchhi and H.M. Van Driel, IEEE Journal of Quantum Electronics, QE-22, 101-107, (1986).
10. N. F. Mott and R. W. Gurney, "Electronic Processes in Ionic Crystals," Oxford Press:New York, (1940).
11. M. A. Lampert and P. Mark, "Current Injection in Solids," Academic Press: New York, (1970), p. 22.
12. S.M. Ryvkin, "Photoelectric Effects in Semiconductors," Consultants Bureau: New York, (1964), p. 186.
13. J. I. Pankove, M. A. Lampert, and M. L. Tarng, Applied Physics Letters, 32, 439, (1978).
14. J. I. Pankove, D. E. Carlson, J. E. Berkeyheiser, and R. O. Wance, Physical Review Letters, 51, 2224, (1983).
15. W. L. Hansen, S. J. Pearton, and E. E. Haller, Applied Physics Letters, 44, 606, (1984).

16. C. T. Sah, J. Y. Sun, and J. J. Tzou, Applied Physics Letters, 43, 204, (1983).
17. N. M. Johnson, C. Herring, and D. J. Chadi, Physical Review Letters, 56, 769, (1986).
18. J. L. Benton, C. J. Doherty, S. D. Ferris, D. L. Flamm, L. C. Kimerling, and H. J. Leamy, Applied Physics Letters, 36, 670, (1980).
19. S. J. Pearton and A. J. Tavendale, Physical Reviews B, 26, 7105, (1982).
20. S. J. Pearton and A. J. Tavendale, Journal of Applied Physics, 54, 1375, (1983).
21. C.H. Seager and D.S. Ginley, Applied Physics Letters, 34, 337-340, (1979).
22. C. H. Seager and D. S. Ginley, Journal of Applied Physics, 52, 1050, (1981).
23. G. P. Pollack, W. F. Richardson, S. D. S. Malhi, T. Binifield, H. Shchijo, S. Banerjee, M. Elahy, A. H. Shah, R. Womack, and P. K. Chatterjee, IEEE Electron Device Letters, EDL 5, 468, (1984).
24. S. J. Pearton, Applied Physics Letters, 40, 253, (1982).
25. H. Fritzche, M. Tanielian, C. C. Tsai, and P. J. Gaczi, Journal of Applied Physics, 50, 3366, (1979).
26. T. R. Hayes, W. C. Dautremont-Smith, H. S. Luftman, and J. W. Lee, Applied Physics Letters, 55, 56, (1989).
27. L. Pavesi, D. Martin, and F. K. Reinhart, Applied Physics Letters, 55, 475, (1989).
28. R. Tsu, E. H. Nicolian, and A. Reisman, Applied Physics Letters, 55, 1897, (1989).
29. S. Albin and L. Watkins, IEEE Electron Device Letters, EDL-11, 159, (1990).

[illegible]

Printed
in USA